THE JOURNAL OF BIOLOGICAL CHEMISTRY VOL. 287, NO. 13, pp. 10325–10343, March 23, 2012

Externalized Glycolytic Enzymes Are Novel, Conserved, and Early Biomarkers of Apoptosis*[S]

Received for publication, October 19, 2011, and in revised form, December 23, 2011 Published, JBC Papers in Press, January 18, 2012, DOI 10.1074/jbc.M111.314971

David S. Ucker[‡1], Mohit Raja Jain[§¶], Goutham Pattabiraman[‡], Karol Palasiewicz[‡], Raymond B. Birge[¶], and Hong Li[§¶2]

From the [‡]Department of Microbiology and Immunology, University of Illinois College of Medicine, Chicago, Illinois 60612 and the [§]Center for Advanced Proteomics Research and [¶]Department of Biochemistry and Molecular Biology, UMDNJ-New Jersey Medical School Cancer Center, Newark, New Jersey 07214

Background: Apoptotic cell recognition triggers profound immunosuppressive responses; relevant recognition determinants are uncharacterized.
Results: Surface exposure of glycolytic enzymes is a common early apoptotic event.
Conclusion: Externalized glycolytic enzyme molecules are novel apoptotic biomarkers and candidate immunomodulatory/recognition determinants.
Significance: Apoptotic glycolytic enzyme externalization explicates plasminogen binding to mammalian cells and potential mechanisms of immune privilege by commensal bacteria and pathogens.

The intriguing cell biology of apoptotic cell death results in the externalization of numerous autoantigens on the apoptotic cell surface, including protein determinants for specific recognition, linked to immune responses. Apoptotic cells are recognized by phagocytes and trigger an active immunosuppressive response ("innate apoptotic immunity" (IAI)) even in the absence of engulfment. IAI is responsible for the lack of inflammation associated normally with the clearance of apoptotic cells; its failure also has been linked to inflammatory and autoimmune pathology, including systemic lupus erythematosus and rheumatic diseases. Apoptotic recognition determinants underlying IAI have yet to be identified definitively; we argue that these molecules are surface-exposed (during apoptotic cell death), ubiquitously expressed, protease-sensitive, evolutionarily conserved, and resident normally in viable cells (SUPER). Using independent and unbiased quantitative proteomic approaches to characterize apoptotic cell surface proteins and identify candidate SUPER determinants, we made the surprising discovery that components of the glycolytic pathway are enriched on the apoptotic cell surface. Our data demonstrate that glycolytic enzyme externalization is a common and early aspect of cell death in different cell types triggered to die with distinct suicidal stimuli. Exposed glycolytic enzyme molecules meet the criteria for IAI-associated SUPER determinants. In addition, our characterization of the apoptosis-specific externalization of glycolytic enzyme molecules may provide insight into the significance of previously reported cases of plasminogen binding to α-enolase on mammalian cells, as well as mechanisms by which commensal bacteria and pathogens maintain immune privilege.

Apoptosis is the primary mechanism by which cells die physiologically and is ongoing throughout life in multicellular organisms. A surprising array of cellular components comprising autoantigens are exposed on the surface of apoptotic cells (1). Apoptotic cells are cleared rapidly *in vivo*; that this phagocytic clearance occurs in the absence of inflammation has long been recognized (2). The clearance of apoptotic cells is a key homeostatic process and represents a final step of the physiological cell death program (3, 4). The failure to promptly clear apoptotic cells even has been linked to chronic inflammation and autoimmunity characteristic of systemic lupus erythematosus, rheumatoid arthritis, and other pathologies, including atherosclerosis (5–8). Independent of phagocytosis, specific apoptotic recognition elicits a profound repertoire of affirmative signaling and effector responses in macrophages and neighboring cells associated generally with the suppression of inflammation and immune responsiveness; we have termed this "innate apoptotic immunity" (4, 9, 10). It may be that the autoimmune pathologies observed in association with the persistence of apoptotic corpses are consequences of deficits in recognition-specific non-phagocytic responses (11).

The anti-inflammatory effects elicited upon the specific recognition of apoptotic cells (12) result primarily from the triggering of transcriptional responses (especially the repression of inflammatory cytokine gene expression) in cells (both professional and non-professional phagocytes) that interact with them (10, 13). Subsequent responses, including the production of anti-inflammatory cytokines (*e.g.* TGF-β and IL-10), extend and may enhance the anti-inflammatory state (14). Although numerous molecules have been implicated in the process of apoptotic cell clearance (15), the critical determinants involved in the recognition of apoptotic cells and in the triggering of functional responses to them remain undefined. Our studies have demonstrated that these determinants are evolutionarily

* This work was supported in part by National Institutes of Health Grants AG029633 (to D. S. U.) and NS046593 (to H. L., for the support of a UMDNJ Neuroproteomics Core Facility).
[S] This article contains supplemental Figs. 1 and 2 and Table I.
[1] To whom correspondence may be addressed: Dept. of Microbiology and Immunology (MC 790), University of Illinois College of Medicine, 835 South Wolcott, Chicago, IL 60612. Tel.: 312-413-1102; Fax: 312-413-7385; E-mail: duck@uic.edu.
[2] To whom correspondence may be addressed: Dept. of Biochemistry and Molecular Biology, UMDNJ-NJMS, 205 S. Orange Ave., CC F1226, Newark, NJ 07103. Tel.: 973-972-8396; Fax: 973-972-1865; E-mail: liho2@umdnj.edu.

conserved and become membrane-exposed during the process of apoptotic cell death without a requirement for ensuing new gene expression (10, 13). Here, we add to this characterization and show that they are protease-sensitive. We note that determinants for apoptotic immune recognition and for the phagocytosis of apoptotic cells may not be identical; for example, phosphatidylserine has been implicated functionally in engulfment (16) and not in innate apoptotic recognition (12, 13).

In an effort to understand the molecular basis for innate immune responses to apoptotic cells, we have taken a comprehensive approach toward the identification of the determinants of apoptotic recognition. We have employed two distinct proteomic approaches based on two-dimensional electrophoretic separations and on isobaric tagging for relative and absolute quantification (iTRAQ),[3] and we have exploited apoptotic membrane vesicles as an enriched source of apoptotic recognition determinants. From our analyses, we identified a large number of over- and underrepresented proteins in apoptotic vesicles. We categorized the identified molecules according to previously assigned molecular functions. Notably, these independent approaches both led to the novel observation that numerous components of the glycolytic pathway are enriched on the apoptotic cell surface. Through cytofluorometric analyses, we have confirmed the apoptosis-associated surface exposure of glycolytic enzymes. Moreover, we have extended these findings to reveal that externalization of glycolytic enzymes is a common attribute of apoptotic cell death, occurring independently of the particular suicidal stimulus and in a variety of cells of different tissue types and species of origin.

Although we have not completed our evaluation of all externalized glycolytic enzyme molecules as determinants of innate apoptotic responses, it is clear that surface-exposed glycolytic enzyme molecules represent novel, early, and unambiguous markers (biomarkers) of the apoptotic cell death process. Surface exposure of glycolytic enzymes has been noted previously in a variety of enteric bacteria and pathogens and is responsible for specific plasminogen binding (17–27). This striking commonality of glycolytic enzyme externalization raises the possibility that the exposure of glycolytic enzymes on microorganisms reflects a subversion of innate apoptotic immunity though apoptotic mimicry that facilitates commensalism or pathogenesis. In this light, it may be appropriate to reevaluate the significance of reported plasminogen-binding activities of glycolytic enzymes.

EXPERIMENTAL PROCEDURES

Cells and Death Induction—Primary murine splenocytes (from C57BL/6 mice), S49 murine thymoma cells, DO11.10 murine T cell hybridomas, RAW 264.7 murine macrophages, Jurkat human T leukemia cells, and U937 human monocytic (histiocytic) leukemia cells were cultured at 37 °C in a humidified 5% (v/v) CO_2 atmosphere in RPMI 1640 medium (Mediatech, Herndon, VA) supplemented with heat-inactivated 10% (v/v) FBS (HyClone Laboratories, Logan, UT), 2 mM L-glutamine, and 50 μM 2-mercaptoethanol. HeLa human cervical carcinoma cells and B2 cells, a transfectant reporter clone of 293T human transformed kidney epithelial cells (13), were grown in DMEM with 4.5 g/liter glucose (Mediatech) supplemented with 10% (v/v) FBS and 2 mM L-glutamine. Physiological cell death (apoptosis) was induced by treatment of cells with the macromolecular synthesis inhibitor actinomycin D (200 ng/ml, 12 h) (28), by irradiation (20 mJ/cm^2) with UVC (254 nm) light, or with staurosporine (1 μM in serum-free medium for 3 h). Autophagy was induced by serum starvation with L-canavanine (1 mM) in the presence of the pan-caspase inhibitor quinolyl-valyl-aspartyl-difluorophenoxy methyl ketone (10 μM; R&D Systems, Minneapolis, MN) and was confirmed by the development of LC3-GFP puncta in transfected cells (29). Pathological cell death (necrosis) was triggered by incubation of cells at 56 °C for 10–20 min (until trypan blue uptake indicated compromise of membrane integrity). Iron-depleted medium was prepared by treatment with Chelex 100 resin (Bio-Rad) as described (30). In some experiments, apoptotic and viable target cells were digested with 0.1% (w/v) trypsin (Sigma) in PBS at 37 °C for 15 min and/or fixed by incubation with 125 mM formaldehyde (Polysciences, Inc., Warrington, PA) in PBS at 25 °C for 20 min as described previously (13).

Vesicles—Plasma membrane vesicles were prepared from HeLa cells as described previously (13). Monolayers of cells, either untreated or induced to die for 4 h with actinomycin D (and still adherent), were stimulated to vesiculate by incubation at 37 °C in vesiculation buffer (10 mM HEPES (pH 7.4), 150 mM NaCl, 2 mM $CaCl_2$, 2 mM DTT, and 25 mM formaldehyde). Supernatants were collected after ~2.5 h (when abundant small membrane vesicles were apparent in the culture fluid). Nonadherent cells were removed by centrifugation at 1000 × *g* for 10 min at 4 °C, and vesicles were pelleted from the cleared supernatant by centrifugation at 30,000 × *g* for 60 min at 4 °C. Cytofluorometric analysis indicated that vesicles were ~0.8 μm in diameter and that the level of contaminating intact cells was less than one cell/100 vesicles. Viable vesicles are comparable in size. Protein content was determined by the Bradford method (Bio-Rad); phospholipid content was quantified by the method of Rouser *et al.* (31).

Cytofluorometric Analyses—For staining with primary antibodies conjugated to FITC or phycoerythrin (PE) or for staining with FITC-conjugated plasminogen (BioMac, Leipzig, German), cells were washed twice with cold PBS containing FBS (1%) before resuspension and staining in the same buffer for 40 min at 4 °C in the dark prior to washing and cytofluorometric analysis. Staining involving unconjugated primary antibodies followed the same procedure and was followed by a second incubation with an appropriate FITC- or PE-conjugated secondary antibody. The vendors of the antibodies and staining reagents used are Abcam (Cambridge, MA), BD Biosciences, Enzo Life Sciences (Farmingdale, NY), Novus Biologicals (Littleton, CO), and Santa Cruz Biotechnology (Santa Cruz, CA).

The accessibility of phosphatidylserine was revealed by the binding of FITC- or PE-conjugated annexin V (BD Biosciences). Cells that had been washed twice with PBS were resus-

[3] The abbreviations used are: iTRAQ, isobaric tagging for relative and absolute quantification; PE, phycoerythrin; 7-AAD, 7-aminoactinomycin D; MFI, mean fluorescence intensity; EnoA, α-enolase; TPI, triose-phosphate isomerase.

pended in 100 μl of annexin V binding buffer (10 mM HEPES (pH 7.4), 150 mM NaCl, and 2.5 mM $CaCl_2$) and incubated with 5 μl of the conjugated annexin V for 40 min in the dark at 25 °C. Propidium iodide and 7-aminoactinomycin D (7-AAD) were employed to assess plasma membrane integrity. Propidium iodide (λ_{ex} = 488 nm and λ_{em} = 610 nm) or 7-AAD (λ_{ex} = 488 nm and λ_{em} = 647 nm) was added to cells (at final concentrations of 1 or 4 μg/ml, respectively) immediately before cytofluorometric analysis.

For intracellular staining, cells were washed twice with cold PBS and fixed and permeabilized in a solution of 4% formaldehyde and 0.1% and saponin in PBS for 30 min at 4 °C in the dark. After fixation, cells were washed twice with PBS buffer containing 0.1% saponin and 1% FBS and stained in this same buffer.

Cells were analyzed cytofluorometrically on a FACSCalibur instrument (BD Biosciences). The excitation wavelength (λ_{ex}) in all cases was at 488 nm. The fluorescence emission wavelength (λ_{em}) from fluorescein was collected at 530 ± 15 nm, from propidium iodide and PE at 610 ± 15 nm, and from 7-AAD at 650 ± 20 nm. Cytofluorometric data were processed with WinMDI software (Joe Trotter, The Scripps Research Institute, La Jolla, CA) or Summit version 4.3 software (Dako, Carpentaria, CA). Where appropriate, fluorescence data are expressed as mean fluorescence intensity (MFI). Attributes of cell death, including changes in forward-angle and side-angle light scatter, were also evaluated as described previously (12).

Transcriptional Modulation—Apoptotic immunosuppressive activity was assessed with respect to NF-κB-dependent transcription utilizing a clone of the B2 reporter cell line (B2.1) as described previously (13).

Protein Identification by Two-dimensional Gel Electrophoresis—Vesicles were lysed by sonication in isoelectric focusing rehydration buffer (7 M urea, 2 M thiourea, 4% CHAPS, 100 mM DTT, 0.2% Bio-Lyte (pH 5–8), 0.01% bromphenol blue, and protease inhibitor). Seventy-five μg of protein in a total of 185 μl of rehydration buffer was applied to 11-cm Bio-Rad Ready-Strip immobilized pH gradient strips (pH 5–8) for overnight rehydration. First-dimension isoelectric focusing was carried out on a Bio-Rad PROTEAN isoelectric focusing system for a total focusing time of 75,000 V-h. After focusing, strips were equilibrated with equilibration buffer I (6 M urea, 0.375 M Tris-HCl (pH 8.8), 2% SDS, 20% glycerol, and 2% (w/v) DTT) for 15 min. The strips were further equilibrated with equilibration buffer II (6 M urea, 0.375 M Tris-HCl (pH 8.8), 2% SDS, 20% glycerol, and 2.5% (w/v) iodoacetamide) for 15 min and directly applied to a 12.5% isocratic SDS-polyacrylamide gel for the second dimension. The resulting gel was then fixed in 10% acetic acid and 40% ethanol for 30 min and stained overnight with SYPRO Ruby. Gels were destained with 10% methanol and 7.5% acetic acid for 60 min. After washing with water, gels were scanned on a 9400 Typhoon variable mode imager (GE Healthcare) using a green laser (532 nm) and 610BP30 emission filter. Quantitative analysis of spots on gels was performed using PDQuest (Bio-Rad) and visually confirmed.

Protein spots from SYPRO Ruby-stained gels were picked for protein identification. The gel spots were diced into 1-mm^3 pieces and washed with 30% acetonitrile in 50 mM ammonium bicarbonate prior to DTT reduction and iodoacetamide alkylation. Trypsin was used for overnight digestion at 37 °C. The resulting peptides were extracted with 30 μl of 1% trifluoroacetic acid, followed by desalting with ZipTip C_{18} pipette tips (Millipore, Bedford, MA). For MS analysis, the peptides were mixed with 7 mg/ml α-cyano-4-hydroxycinnamic acid matrix (in 60% acetonitrile) in a 1:1 ratio and spotted onto a MALDI plate. The peptides were analyzed on a 4800 MALDI TOF/TOF analyzer (Applied Biosystems, Framingham, MA). Mass spectra (m/z 880–3200) were acquired in positive ion reflector mode. The 15 most intense ions were selected for subsequent MS/MS sequencing analysis in 1-keV mode. Protein identification was performed by searching the combined MS and MS/MS spectra against the human NCBI database using a local MASCOT search engine (version 1.9) on a GPS server (version 3.5, Applied Biosystems). Proteins containing at least two peptides identified with confidence interval values of no less than 95% were considered as being identified.

Protein Quantification by iTRAQ Analysis—For iTRAQ labeling, proteins from vesicles were extracted in iTRAQ lysis buffer (1% Nonidet P-40, 1% Triton X-100, 10 mM HEPES, and 500 mM triethylammonium bicarbonate buffer) using probe sonication at 50% duty for three cycles of 15 s with a 60-s incubation in ice-cold water between cycles. The lysate was cleared by centrifugation at 16,100 × g for 15 min. The pH of samples was adjusted to 8.0 with 1.0 M triethylammonium bicarbonate buffer. The iTRAQ labeling procedures were performed according to the manufacturer's instructions as further described (32). Briefly, after reduction with tris(2-carboxyethyl)phosphine hydrochloride and alkylation with methyl methanethiosulfonate, tryptic digestion of each sample (100 μg) was initiated by the addition of 10 μg of trypsin (Promega, Madison, WI), and each sample was incubated overnight at 37 °C. Peptides derived from viable samples were labeled with iTRAQ tags 114 and 115, whereas peptides derived from apoptotic samples were labeled with iTRAQ tags 116 and 117. The labeled samples were then mixed together and fractionated via strong cation exchange and reverse phase chromatography according to a procedure described previously (33). The HPLC eluate was mixed with a matrix solution (7 mg/ml α-cyano-4-hydroxycinnamic acid in 60% acetonitrile, 5 mM ammonium monobasic phosphate, and internal mass calibrants (50 fmol/μl each [Glu^1]fibrinopeptide B and ACTH(18–39)) through a 30-nl mixing tee and directly spotted onto the MALDI plates. The peptides were analyzed on a 4800 Proteomics Analyzer MALDI TOF/TOF tandem mass spectrometer (Applied Biosystems) in a data-dependent fashion using job-wide interpretation. MS spectra (m/z 800–3600) were acquired in positive ion reflectron mode with internal mass calibration. A maximum of the 15 most intense ions (signal-to-noise ratio > 50) per spot were selected for subsequent MS/MS analysis in 1.0-keV mode. Each spectrum was averaged over 2000 laser shots.

Protein Database Search and Bioinformatics—TS2Mascot (Matrix Science Inc., Boston, MA) was used to generate peak lists in Mascot generic file format from the MS/MS spectra using the following parameters: mass range from 20 to 60 Da below precursor and signal-to-noise ratio ≥ 10. The peak lists was submitted for automated search using a local Mascot server (version 2.2) against 20,244 proteins in the Swiss-Prot human

protein sequence database. The following parameters were used for the search: iTRAQ 4plex (K), iTRAQ 4plex (N-terminal), and methylthio (C) as fixed modifications; iTRAQ 4plex (Y) and oxidation (M) as variable modifications; trypsin as the digestive enzyme with up to two missed cleavages allowed; monoisotopic mass with peptide precursor mass tolerance of 50 ppm; and MS/MS ion mass tolerance of 0.3 Da. Scaffold (version 3_03_01, Proteome Software Inc., Portland, OR) was used to filter MS/MS-based peptide and protein identifications. Peptide identifications were accepted if they could be established at or greater than 95.0% probability and ≤1.0% false discovery rate as specified by the Peptide Prophet algorithm (34). Protein identifications were accepted if they could be established at or greater than 95.0% probability and contained at least one identified peptide at 95% confidence. Protein probabilities were assigned by the Protein Prophet algorithm (35). Proteins that contained similar peptides and could not be differentiated based on MS/MS analysis alone were grouped to satisfy the principles of parsimony. Peptides were quantified using the centroided iTRAQ reporter ion peak intensity. Protein quantitative values were derived from only uniquely assigned peptides. Protein quantitative ratios were calculated as the median of all relevant peptide ratios for each protein. A log 2-fold ratio for each protein reported by Scaffold was transformed to normal relative protein abundance -fold ratios in Excel (Microsoft, Redmond, WA). A two-tailed *t* test was performed using Excel for final statistical evaluation. In addition, only proteins altered in abundance by at least 20% from the viable vesicles were considered significant. For each identified protein, associated gene ontology terms were automatically fetched from the European Bioinformatics Institute by Scaffold software and plotted with respect to enrichment.

Enzyme Assays—Enolase activity was assessed as the fluoride-inhibitable (36) conversion of 2-phosphoglycerate to phosphoenolpyruvate by a modification of an assay described by Pancholi and Fischetti (20). Intact viable and apoptotic HeLa cells were washed once with 1× PBS. Graded numbers of cells (ranging from 1×10^6 to 3×10^4) were added to a 200-μl reaction in enolase buffer (10 mM $MgCl_2$ in 1× PBS). Reactions were started with the addition of 2-phosphoglycerate (to a final concentration of 3 mM). After 4 min of incubation at 25 °C, reactions were terminated by the addition of 800 μl of enolase stop buffer (10 mM $MgCl_2$ and 3 mM NaF in 1× PBS). Cells were removed by centrifugation at 600 × *g* for 5 min, and phosphoenolpyruvate in supernatants was quantified spectrophotometrically (λ = 240 nm). The molar extinction coefficient of phosphoenolpyruvate at 240 nm is 1.164×10^3. Enolase activity in cell extracts (comparably graded cell equivalents) was assessed similarly. Extracts were prepared from viable and apoptotic HeLa cells by sonication for 6 × 10 s at 60 watts (Vibra-Cell sonicator, Sonics and Materials, Danbury, CT) after allowing the cells to swell on ice in 0.1× PBS for 30 min. Enolase activity in cell supernatants was assessed after incubating graded numbers of intact cells (as described above) in mock reactions in enolase buffer without 2-phosphoglycerate. After 4 min, cells were removed by centrifugation. 2-Phosphoglycerate was then added to the supernatant, and the 2-phosphoglycerate-dependent production of phosphoenolpyruvate was assessed after 4 min as described above.

The determination of GAPDH activity followed a similar set of procedures and was assessed as the conversion of NAD to NADH dependent on glyceraldehyde 3-phosphate by a modification of an assay described by Pancholi and Fischetti (17). In particular, the reaction buffer was adjusted to iso-osmolarity. Graded numbers of intact, washed, apoptotic, and viable HeLa cells (ranging from 3×10^5 to 1×10^4) were added to a 200-μl reaction in GAPDH buffer (60 mM NaCl, 50 mM Na_2HPO_4, 40 mM triethanolamine, and 1 mM NAD (pH 8.6)). Reactions were started by the addition of glyceraldehyde 3-phosphate to a final concentration of 2 mM. After 4 min of incubation at 25 °C, reactions were terminated by the addition of 800 μl of GAPDH stop buffer (60 mM NaCl, 50 mM Na_2HPO_4, and 40 mM triethanolamine (pH 10.0)). Cells were removed by centrifugation, and NADH in supernatants was quantified spectrophotometrically (λ = 340 nm). The molar extinction coefficient of NADH at 340 nm is 6.22×10^3.

RESULTS

Apoptotic Suppressive Determinants, Enriched in Membrane Vesicles, Are Protease-sensitive—We have demonstrated that apoptotic determinants for recognition and immune modulation are evolutionarily conserved and arise on the surface of cells during the process of apoptotic death without a requirement for ensuing new gene expression (10, 12). The ability of apoptotic cells to modulate inflammatory responses occurs primarily at the level of transcription (10) and can be assessed reliably with transcriptional reporters that disclose primary inflammatory responses (*i.e.* transcriptional promoters linked to the firefly luciferase gene and responsive to critical transcriptional activators involved in inflammatory responses, such as NF-κB) (10, 13). Fig. 1 provides examples of the specific dose-dependent effects of apoptotic cells on a responsive cell line harboring such a transcriptional reporter. B2.1 is a highly responsive clone of stably transfected human HEK293T reporter cells (13). The results show that apoptotic cells repressed NF-κB-dependent transcription, whereas viable cells did not and recapitulated cytokine responses of those cells (13). Importantly, apoptotic cells of distinct species and tissues of origin (S49 (in Fig. 1*A*) is a murine T lymphocyte cell line, and HeLa (in Fig. 1*B*) is a human epithelial cell line) triggered equivalent responses.

Previously, we found that the phospholipid phosphatidylserine is neither a sufficient determinant (12) nor a necessary component (13) for specific apoptotic recognition and immune modulation. We wondered whether apoptotic immunosuppressive activity involves protein determinants and would therefore be susceptible to proteolytic digestion. Indeed, we found that when apoptotic cells were digested with trypsin, their immunomodulatory activity was lost (Fig. 1*A*). Interestingly, we found that upon extended incubation following tryptic digestion, apoptotic cells recovered modulatory activity (data not shown). Fixation with formaldehyde after protease treatment precludes this recovery, although apoptotic immunomodulatory activity is stable to fixation with formaldehyde (13). We interpret these results to suggest that apoptotic immu-

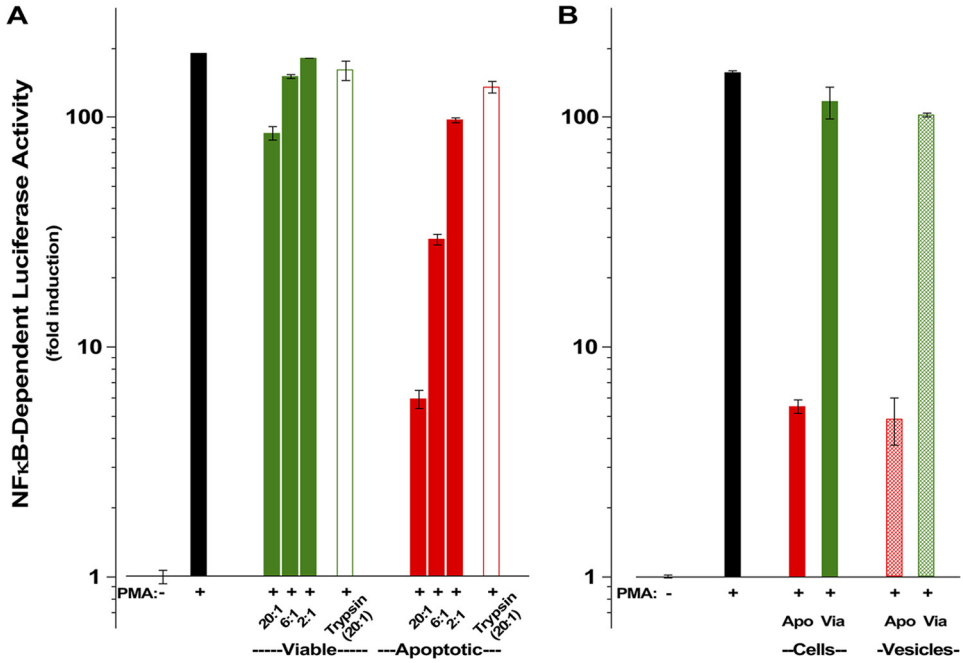

FIGURE 1. **Apoptotic suppressive determinants are protease-sensitive and enriched in membrane vesicles.** Apoptotic suppression of NF-κB-dependent transcription was assessed with respect to NF-κB-dependent luciferase activity in B2.1 reporter cells (13). *A*, suppression of phorbol 12-myristate 13-acetate (*PMA*; 1.25 ng/ml)-induced NF-κB-dependent luciferase activity by graded numbers (indicated as the target/responder ratio) of viable (*Via*; *green*) or apoptotic (*Apo*; actinomycin D, 200 ng/ml; *red*) S49 murine T cells (*closed bars*) and targets that had been digested with trypsin (0.1%, 15 min, 37 °C; *open bars*) was assessed. Trypsin was removed from targets by extensive washing, and residual activity was quenched by incubation in 10% serum-containing medium. *B*, human epithelial (HeLa) cell targets were left untreated or treated with actinomycin D. The suppressive activity of cells (*closed bars*; target/responder ratio = 8:1) and vesicles (*hatched bars*; target/responder ratio = 30:1), prepared by incubation of untreated and treated cells in vesiculation buffer (see "Experimental Procedures"), was assessed independently as described for *A*.

nomodulatory determinants are protease-sensitive molecules (or molecular complexes including essential protein components) that are resident in all cells prior to cell death and that some fraction of the intracellular stores of the relevant molecules becomes surface-exposed (and susceptible to tryptic digestion) due to apoptosis-specific post-translational modification. For brevity, the acronym SUPER (surface-exposed (during apoptotic cell death), ubiquitously expressed, protease-sensitive, evolutionarily conserved, and resident normally in viable cells) serves to emphasize these defining properties of apoptotic determinants for recognition and immune modulation.

We have shown that membrane vesicles prepared from apoptotic cells expose these determinants (13). In fact, assays for specific NF-κB-dependent transcriptional suppression as a function of the dose of apoptotic vesicles reveal that apoptotic membrane vesicles are enriched in immunomodulatory determinants, relative to whole apoptotic cells and comparable vesicles prepared from viable cells. As shown in Fig. 1*B*, titration of the immunomodulatory activity of intact apoptotic HeLa cells and apoptotic vesicles prepared from them demonstrated that vesicles have ~25% of the immunomodulatory activity of whole cells. (The low level at which whole cells contaminate vesicle preparations does not account for this activity.) Given that the surface area of whole cells is ~125-fold greater than that of these vesicles (we estimate the ratio of surface areas as $4\pi r_c^2/4\pi r_v^2 \cong 500$, where r_c (the radius of an intact HeLa cell) is ~9 μm and r_v (the average radius of a vesicle) is 0.8 μm) and that the membrane-associated protein content/nmol of phospholipid of a vesicle is ~30-fold greater than that of a whole cell (4.70 μg of protein/nmol of phospholipid for intact cells *versus* 0.15 μg of protein/nmol of phospholipid for vesicles), we calculate the vesicle enrichment of immunomodulatory protein determinants to be ~1000-fold (*i.e.* $0.25 \times 125 \times 30 = 938$).

Proteomic Analyses of Apoptotic Membrane Vesicles Reveal Membrane Association of Glycolytic Enzyme Molecules—The implication that determinants of innate apoptotic immunity necessarily include essential protein components and that membrane vesicles provide an enriched source of those determinants led us to undertake a systematic analysis of the proteome of apoptotic plasma membrane vesicles. We performed a comparative analysis of membrane vesicle proteins prepared from apoptotic and viable cells by two-dimensional gel electrophoresis (Fig. 2 and Table 1). After electrophoretic resolution, spots of proteins that were distinctly altered in abundance (over- or underrepresented) were excised and subjected to tryptic digestion, followed by nanoflow LC and MS/MS analysis.

Interestingly, among the most prominent of the overrepresented species we observed were proteins known to be involved as enzymes in the terminal stages of glucose metabolism, including pyruvate kinase (Fig. 2, highlighted in *blue*), α-enolase (EnoA; shown in *magenta*), and triose-phosphate isomerase (TPI; shown in *green*). Each of these proteins was identified in multiple gel spots (with distinct pI values), and the abundance of each of the distinct spots was found to be increased among proteins from the apoptotic (relative to viable) membrane vesicles (Fig. 2). The multiple spots may be indicative of isoforms of each of these proteins harboring post-translational modifications. Notably, apoptosis-associated proteolysis does not appear generally to underlie these modifications; only in the

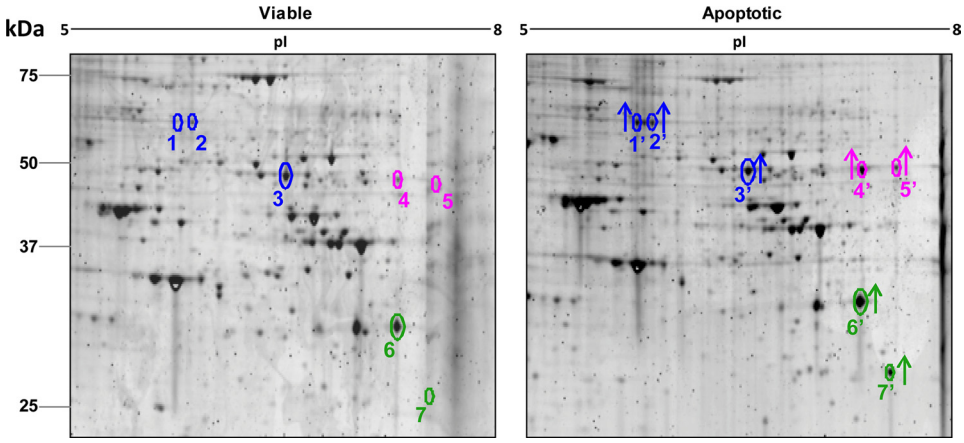

FIGURE 2. **Analysis of membrane vesicle proteins by two-dimensional gel electrophoresis.** Shown are the results from comparative analysis of membrane vesicle preparations from viable and apoptotic HeLa cells by two-dimensional gel electrophoresis. Multiple gel spots corresponding to pyruvate kinase (*blue*), EnoA (*magenta*), and TPI (*green*) are indicated. The increased abundance of protein spots among apoptotic (relative to viable) membrane vesicles is indicated by *arrows*. Details are listed in Table 1.

TABLE 1
Isoforms of identified membrane proteins

Protein	Apparent molecular mass	Apparent pI	Ratio[a]
	kDa		
Pyruvate kinase[b]			
Spots 1 and 1′	~58	~5.7	1.9
Spots 2 and 2′	~58	~5.8	1.3
Spots 3 and 3′	~48	~6.5	1.1
EnoA[c]			
Spots 4 and 4′	~48	~7.1	2.1
Spots 5 and 5′	~48	~7.5	1.4
TPI[d]			
Spots 6 and 6′	~31	~7.1	1.2
Spots 7 and 7′	~26	~7.3	3.6

[a] The ratio of normalized densitometric intensities of a spot in the apoptotic sample to the comparable viable spot was determined.
[b] Predicted molecular mass of 58 kDa and pI 7.96 (104).
[c] Predicted molecular mass of 47 kDa and pI 7.01 (105).
[d] Predicted molecular mass of 31 kDa and pI 5.65 (106).

case of TPI (*spot 7′*) is an apoptosis-enriched isoform of distinctly lower apparent molecular mass (presumably due to proteolytic cleavage) evident.

Independently, we undertook a complete quantitative proteomic characterization of apoptotic and viable membrane vesicles employing iTRAQ technology, which permits the analysis of less abundant species. Apoptotic and viable vesicle extracts were denatured, alkylated, and labeled with isobaric iTRAQ reagent tags (see "Experimental Procedures"). Duplicate viable vesicle peptides were labeled with iTRAQ reagent tags 114 and 115 (differential tags of 114 and 115 Da, respectively); duplicate apoptotic membrane peptides were labeled with iTRAQ tags 116 and 117. Samples were then digested with trypsin, and the labeled peptides were mixed in even ratios and quantified by LC-MS/MS. The relative abundance (enrichment or depletion) of distinct peptides in apoptotic and viable samples was determined by replicate comparisons between the labeled samples. From these data, we identified a total of 564 proteins (supplemental Table I). A graphic representation of this distribution, highlighting selected proteins, is shown in Fig. 3. Tables 2 and 3 list 56 overrepresented and 105 underrepresented proteins, respectively, that varied by at least 20% between apoptotic and viable membrane vesicle preparations at a false discovery rate of <1%. We have previously established, with known standards, that the analytical coefficient of variance is <10%; therefore, changes between apoptotic and viable membrane proteins of >20% are reliably significant. Notably, the overrepresented population included proteins from all intracellular locales (see below).

With the vesiculation protocol, as many as 8% of the cells in an otherwise untreated control ("viable") cell culture become apoptotic. Thus, we would expect that an idealized candidate SUPER molecule (*i.e.* a protein that is not associated with viable cell membranes and that is associated specifically with apoptotic cell membranes (and that actually is overrepresented by *x*-fold among apoptotic cell membrane proteins)) would appear to be enriched among apoptotic vesicle proteins by no more than ~12-fold (*i.e.* $x/0.08x$). Although the membrane vesicles that we prepared have no ultrastructure and are depleted for non-membrane-associated molecules, the non-surface-exposed intravesicular contents of viable vesicles may contribute further to a diminution of the apparent enrichment of apoptosis-specific membrane proteins in apoptotic vesicle preparations. Indeed, the maximum enrichment of a protein that we observed among apoptotic vesicles (Fig. 3) was <3-fold.

Inventory of Apoptotic Membrane Proteins—We categorized the identified molecules according to previous descriptions of their major molecular functions (Fig. 4; see below). Molecules characterized for their catalytic activities involved in metabolism constituted the largest group of overrepresented proteins present in apoptotic cell vesicles (15/56). Among these, glycolytic enzymes (including aldolase, TPI, phosphoglycerate kinase, EnoA, and pyruvate kinase) were highly represented, consistent with our two-dimensional gel electrophoresis analysis. An example of this enrichment, observed by iTRAQ analysis, is presented for EnoA peptides (Fig. 5). Indeed, it is striking that almost all members of the glycolytic pathway are enriched among apoptotic cell membranes (see Fig. 3, *inset*). Other major classes among the overrepresented proteins present in apoptotic vesicles are structural (including cytoskeletal) molecules (14/56), those involved in macromolecular synthesis (especially translation) and processing (including proteases) (12/56), and molecular chaperones (7/56).

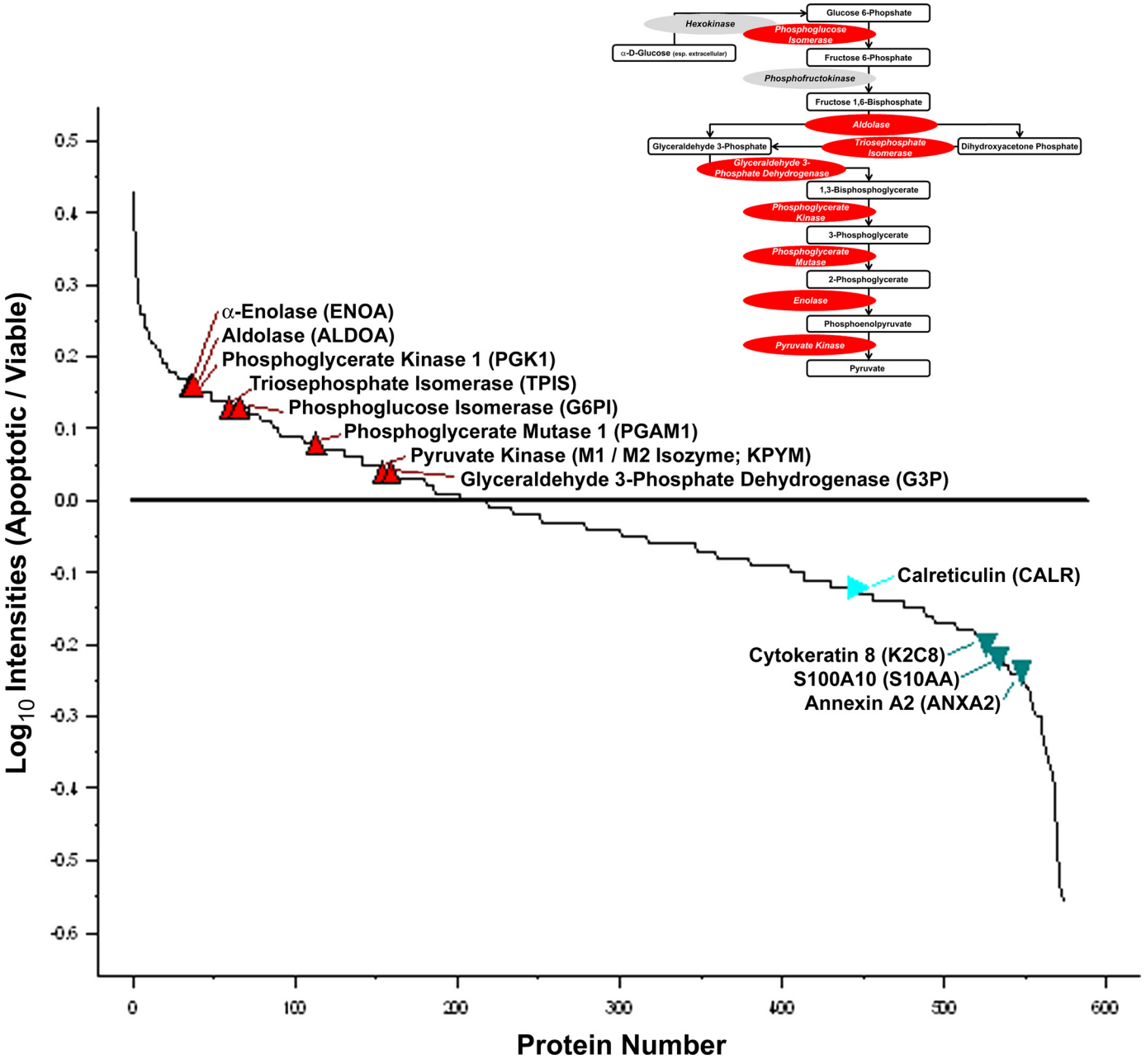

FIGURE 3. **Relative abundance of apoptotic and viable membrane vesicle proteins determined by iTRAQ analysis.** Shown is a compilation of the relative abundance of membrane vesicle proteins from apoptotic *versus* viable preparations (*Apoptotic/Viable*) determined by iTRAQ analysis (see supplemental Table I). The relative abundance of selected proteins is indicated. Proteins involved as enzymes in the glycolytic pathway (see *inset*; shown in *red*) are found to be overrepresented. Other molecules identified as plasminogen receptors (see text; shown in *green*) are underrepresented.

Importantly, some of the proteins identified here as enriched among apoptotic vesicles (for example, the actin-associated proteins cofilin and Arp2/3 (37), numerous heat shock proteins, and other chaperones associated with stress (38–40)) fulfill expectations derived from other studies. Similarly, the mitochondrial protein cytochrome *c* is known to be released from mitochondria during apoptotic cell death (41, 42). It is significant that not all of the vesicle-enriched molecules are membrane-exposed; in particular, we did not detect surface-exposed cytochrome *c* (data not shown).

On the other hand, some proteins expected to be enriched in apoptotic vesicles were not identified in this array. Actin was expected to be among the apoptotic vesicle proteins (43–45), along with actin-associated and other structural molecules. Histones also were expected to be enriched among apoptotic vesicle proteins based on previous studies documenting their unique presence on the apoptotic cell surface (1). The observation that vesicles have immunomodulatory activity (like intact apoptotic cells) but lack externalized histones (unlike intact apoptotic cells) allows us to exclude histones definitively as apoptotic recognition determinants. Annexin A1, which has been suggested previously to be involved in apoptotic recognition (46), was relatively depleted in our apoptotic vesicle preparation (only ~70% representation) (Table 3) relative to the viable vesicle preparation. Other proteomic studies also have not found

TABLE 2

Overrepresented apoptotic membrane-associated proteins

Proteins identified by iTRAQ analysis and found to be overrepresented among apoptotic membrane vesicles by at least 20% at a confidence level of >95% are listed. SUMO, small ubiquitin-like modifier.

Identified proteins	Accession ID	Ratio	*t* test
Cytochrome *c*	CYC_HUMAN	2.71	0.01
Stathmin	STMN1_HUMAN	2.07	0.00
Macrophage migration inhibitory factor	MIF_HUMAN	2.00	0.01
Acyl-CoA-binding protein	ACBP_HUMAN	1.94	0.05
SUMO-conjugating enzyme UBC9	UBC9_HUMAN	1.81	0.02
Profilin-1	PROF1_HUMAN	1.80	0.01
T-complex protein 1 subunit ϵ	TCPE_HUMAN	1.74	0.01
Peptidylprolyl *cis*,*trans*-isomerase A	PPIA_HUMAN	1.74	0.00
Calpastatin	ICAL_HUMAN	1.68	0.03
Glutathione S-transferase Ω1	GSTO1_HUMAN	1.68	0.00
Aldose reductase	ALDR_HUMAN	1.68	0.02
Heat shock protein HSP90α	HS90A_HUMAN	1.68	0.05
Transgelin-2	TAGL2_HUMAN	1.68	0.05
Plastin-3	PLST_HUMAN	1.62	0.01
Nucleoside-diphosphate kinase B	NDKB_HUMAN	1.62	0.03
14-3-3 protein β/α	1433B_HUMAN	1.57	0.02
Thioredoxin	THIO_HUMAN	1.56	0.03
Myristoylated alanine-rich C-kinase substrate	MARCS_HUMAN	1.52	0.05
Importin-7	IPO7_HUMAN	1.52	0.01
Glutathione S-transferase P	GSTP1_HUMAN	1.51	0.02
α-Actinin-1	ACTN1_HUMAN	1.46	0.01
Spectrin β chain, brain 1	SPTB2_HUMAN	1.46	0.01
Cytosolic phospholipase A_2	PA24A_HUMAN	1.46	0.01
ATP synthase subunit d, mitochondrial	ATP5H_HUMAN	1.46	0.01
Nuclear migration protein NudC	NUDC_HUMAN	1.46	0.01
α-Enolase	ENOA_HUMAN	1.46	0.03
Fructose-bisphosphate aldolase A	ALDOA_HUMAN	1.46	0.03
T-complex protein 1 subunit θ	TCPQ_HUMAN	1.46	0.03
Phosphoglycerate kinase 1	PGK1_HUMAN	1.46	0.03
Heat shock cognate 71-kDa protein	HSP7C_HUMAN	1.37	0.01
Actin-related protein 2/3 complex subunit 3	ARPC3_HUMAN	1.37	0.01
Nascent polypeptide-associated complex subunit α	NACA_HUMAN	1.37	0.01
Cu,Zn-superoxide dismutase	SODC_HUMAN	1.36	0.05
Proteasome subunit β type 3	PSB3_HUMAN	1.36	0.05
Triose-phosphate isomerase	TPIS_HUMAN	1.36	0.05
Heat shock protein HSP90β	HS90B_HUMAN	1.36	0.05
14-3-3 protein ϵ	1433E_HUMAN	1.36	0.05
Tyrosyl-tRNA synthetase, cytoplasmic	SYYC_HUMAN	1.36	0.05
Ubiquitin-like modifier-activating enzyme 1	UBA1_HUMAN	1.36	0.05
Ezrin	EZRI_HUMAN	1.32	0.03
Cofilin-1	COF1_HUMAN	1.32	0.03
Transgelin	TAGL_HUMAN	1.32	0.03
Proteasome subunit α type 5	PSA5_HUMAN	1.32	0.00
T-complex protein 1 subunit γ	TCPG_HUMAN	1.32	0.04
L-Lactate dehydrogenase A chain	LDHA_HUMAN	1.32	0.04
Ras-related protein Rab-1B	RAB1B_HUMAN	1.28	0.02
Actin-related protein 2/3 complex subunit 2	ARPC2_HUMAN	1.27	0.02
Eukaryotic peptide chain release factor GTP-binding subunit ERF3A	ERF3A_HUMAN	1.27	0.02
Fatty acid synthase	FAS_HUMAN	1.23	0.00
Protein SET	SET_HUMAN	1.19	0.04
Phosphoglycerate mutase 1	PGAM1_HUMAN	1.19	0.04
Elongation factor 1γ	EF1G_HUMAN	1.19	0.04
Proliferation-associated protein 2G4	PA2G4_HUMAN	1.19	0.03
Elongation factor 2	EF2_HUMAN	1.19	0.03
Acidic leucine-rich nuclear phosphoprotein 32 family member A	AN32A_HUMAN	1.19	0.03
Importin subunit β1	IMB1_HUMAN	1.19	0.03

annexin A1 to be present generally among apoptotic membrane proteins (see, for example, Ref. 47).

It is most striking that both of the independent proteomic analyses we employed identified the preferential membrane vesicle association of glycolytic enzymes with apoptotic cell death. Because the issue of surface exposure is a defining criterion with regard to apoptotic determinants for recognition and immune modulation (SUPER) candidates, we sought to evaluate whether glycolytic enzyme molecules are present on the apoptotic cell surface.

Cytofluorometric Confirmation of Apoptotic Externalization of Glycolytic Enzyme Molecules—We examined independently the preferential enrichment of glycolytic enzyme molecules among apoptotic membrane proteins and tested specifically whether those molecules are exposed on the apoptotic cell surface. We analyzed apoptotic cells for the externalization of three glycolytic enzymes (EnoA, GAPDH, and TPI) by immunofluorescence and cytofluorometric analyses. We examined a variety of cell types and cell lines for cell death-associated externalization of these proteins. (In addition to the HeLa cells used to prepare the membrane vesicles subjected to our protein analyses, we analyzed human and murine epithelial, lymphoid, and myeloid cell lines and primary cells induced to undergo apoptotic death with a variety of suicidal stimuli.)

By immunofluorescence staining analysis, we found that EnoA is displayed generally on the surface of apoptotic (but not viable) cells. An example of these analyses (with primary murine splenocytes) is presented in Fig. 6*A*. Completely analo-

TABLE 3

Underrepresented apoptotic membrane-associated proteins

Proteins identified by iTRAQ analysis and found to be underrepresented among apoptotic membrane vesicles by at least 20% at a confidence level of >95% are listed.

Identified proteins	Accession ID	Ratio	*t* test
Histone H2A type 2B	H2A2B_HUMAN	0.28	0.01
Large neutral amino acids transporter small subunit 1	LAT1_HUMAN	0.29	0.03
Dipeptidyl peptidase 1	CATC_HUMAN	0.31	0.02
Small nuclear ribonucleoprotein-associated proteins B and B′	RSMB_HUMAN	0.32	0.03
Alkaline phosphatase, tissue-nonspecific isozyme	PPBT_HUMAN	0.42	0.03
Asparagine synthetase (glutamine-hydrolyzing)	ASNS_HUMAN	0.42	0.02
60 S ribosomal protein L19	RL19_HUMAN	0.45	0.03
Annexin A5	ANXA5_HUMAN	0.45	0.02
Annexin A6	ANXA6_HUMAN	0.47	0.02
60 S ribosomal protein L24	RL24_HUMAN	0.50	0.02
Cytochrome bc_1 complex subunit 7	QCR7_HUMAN	0.50	0.02
40 S ribosomal protein S17	RS17_HUMAN	0.52	0.00
Keratin, type I cytoskeletal 10	K1C10_HUMAN	0.54	0.04
60 S ribosomal protein L34	RL34_HUMAN	0.56	0.04
40 S ribosomal protein S2	RS2_HUMAN	0.57	0.03
Annexin A2	ANXA2_HUMAN	0.57	0.03
Heat shock protein β1	HSPB1_HUMAN	0.57	0.00
40 S ribosomal protein S23	RS23_HUMAN	0.57	0.01
Protein S100A4	S10A4_HUMAN	0.57	0.03
60 S ribosomal protein L32	RL32_HUMAN	0.58	0.01
Programmed cell death protein 6	PDCD6_HUMAN	0.59	0.03
60 S ribosomal protein L36a	RL36A_HUMAN	0.59	0.00
DNA replication licensing factor MCM5	MCM5_HUMAN	0.60	0.02
60 S ribosomal protein L9	RL9_HUMAN	0.60	0.02
Protein transport protein Sec31A	SC31A_HUMAN	0.60	0.02
Tubulin β4 chain	TBB4_HUMAN	0.60	0.05
Protein S100A10	S10AA_HUMAN	0.61	0.03
Small nuclear ribonucleoprotein SmD3	SMD3_HUMAN	0.61	0.03
Polypeptide *N*-acetylgalactosaminyltransferase 2	GALT2_HUMAN	0.62	0.00
Non-POU domain-containing octamer-binding protein	NONO_HUMAN	0.62	0.01
60 S ribosomal protein L14	RL14_HUMAN	0.62	0.04
Endothelin-converting enzyme 1	ECE1_HUMAN	0.62	0.04
Keratin, type II cytoskeletal 8	K2C8_HUMAN	0.64	0.04
Interleukin enhancer-binding factor 3	ILF3_HUMAN	0.64	0.04
Histone H2B type 1 J	H2B1J_HUMAN	0.64	0.01
DNA replication licensing factor MCM4	MCM4_HUMAN	0.64	0.02
Histone H1.5	H15_HUMAN	0.64	0.02
40 S ribosomal protein S18	RS18_HUMAN	0.66	0.04
Annexin A1	ANXA1_HUMAN	0.66	0.04
60 S ribosomal protein L26	RL26_HUMAN	0.66	0.00
Lysosome-associated membrane glycoprotein 1	LAMP1_HUMAN	0.66	0.01
$\Delta^{3,5},\Delta^{2,4}$-Dienoyl-CoA isomerase, mitochondrial	ECH1_HUMAN	0.66	0.01
Splicing factor, arginine/serine-rich 6	SFRS6_HUMAN	0.66	0.01
Mitochondrial carrier homolog 2	MTCH2_HUMAN	0.66	0.01
Probable ATP-dependent RNA helicase DDX17	DDX17_HUMAN	0.66	0.01
40 S ribosomal protein S16	RS16_HUMAN	0.68	0.05
40 S ribosomal protein S3a	RS3A_HUMAN	0.68	0.05
Clathrin light chain A	CLCA_HUMAN	0.68	0.05
EGF-like repeat- and discoidin I-like domain-containing protein 3	EDIL3_HUMAN	0.68	0.05
Guanine nucleotide-binding protein G(I)/G(S)/G(T) subunit β1	GBB1_HUMAN	0.68	0.05
40 S ribosomal protein S9	RS9_HUMAN	0.68	0.01
N-Acetylgalactosaminyltransferase 7	GALT7_HUMAN	0.68	0.01
40 S ribosomal protein S15a	RS15A_HUMAN	0.68	0.01
Aspartyl-tRNA synthetase, cytoplasmic	SYDC_HUMAN	0.68	0.01
X-ray repair cross-complementing protein 5	XRCC5_HUMAN	0.68	0.03
Interleukin enhancer-binding factor 2	ILF2_HUMAN	0.68	0.03
Protein ERGIC-53	LMAN1_HUMAN	0.69	0.05
60 S ribosomal protein L23	RL23_HUMAN	0.71	0.05
Heterogeneous nuclear ribonucleoproteins A2 and B1	ROA2_HUMAN	0.71	0.00
Peroxiredoxin-2	PRDX2_HUMAN	0.71	0.00
60 S ribosomal protein L13	RL13_HUMAN	0.71	0.02
Reticulon-4	RTN4_HUMAN	0.71	0.02
60 S ribosomal protein L18	RL18_HUMAN	0.71	0.02
60 S ribosomal protein L15	RL15_HUMAN	0.71	0.03
Myosin light polypeptide 6	MYL6_HUMAN	0.73	0.02
60 S ribosomal protein L6	RL6_HUMAN	0.73	0.02
Heterogeneous nuclear ribonucleoproteins C1 and C2	HNRPC_HUMAN	0.73	0.02
60 S ribosomal protein L35	RL35_HUMAN	0.73	0.01
Calumenin	CALU_HUMAN	0.73	0.01
DNA topoisomerase 2α	TOP2A_HUMAN	0.73	0.01
Heterogeneous nuclear ribonucleoprotein G	HNRPG_HUMAN	0.73	0.01
60 S ribosomal protein L3	RL3_HUMAN	0.73	0.05
ADP/ATP translocase 2	ADT2_HUMAN	0.73	0.05
Tubulin β chain	TBB5_HUMAN	0.76	0.00
DNA-dependent protein kinase catalytic subunit	PRKDC_HUMAN	0.76	0.03
40 S ribosomal protein S10	RS10_HUMAN	0.76	0.03
Vigilin	VIGLN_HUMAN	0.76	0.03
60 S ribosomal protein L4	RL4_HUMAN	0.78	0.02
40 S ribosomal protein S19	RS19_HUMAN	0.78	0.02

TABLE 3—*continued*

Identified proteins	Accession ID	Ratio	*t* test
60 S ribosomal protein L10	RL10_HUMAN	0.78	0.02
60 S ribosomal protein L21	RL21_HUMAN	0.78	0.02
60 S ribosomal protein L7a	RL7A_HUMAN	0.78	0.02
Heterogeneous nuclear ribonucleoprotein D0	HNRPD_HUMAN	0.78	0.02
Heterogeneous nuclear ribonucleoprotein R	HNRPR_HUMAN	0.78	0.02
40 S ribosomal protein S4, X isoform	RS4X_HUMAN	0.81	0.05
60 S ribosomal protein L13a	RL13A_HUMAN	0.81	0.05
60 S ribosomal protein L23a	RL23A_HUMAN	0.81	0.05
60 S ribosomal protein L18a	RL18A_HUMAN	0.81	0.05
Heterogeneous nuclear ribonucleoprotein L	HNRPL_HUMAN	0.81	0.05
Serpin H1	SERPH_HUMAN	0.81	0.05
Thymidylate kinase	KTHY_HUMAN	0.81	0.05
Trifunctional enzyme subunit α, mitochondrial	ECHA_HUMAN	0.81	0.05
ATP-dependent RNA helicase A	DHX9_HUMAN	0.84	0.04
26 S protease regulatory subunit 4	PRS4_HUMAN	0.84	0.04
60 S acidic ribosomal protein P0	RLA0_HUMAN	0.84	0.04
Actin-related protein 2	ARP2_HUMAN	0.84	0.04
Cytochrome b_5	CYB5_HUMAN	0.84	0.04
Filamin-A	FLNA_HUMAN	0.84	0.04
Nucleolin	NUCL_HUMAN	0.84	0.04
Signal recognition particle 9-kDa protein	SRP09_HUMAN	0.84	0.04
60 S ribosomal protein L7	RL7_HUMAN	0.84	0.03
40 S ribosomal protein S8	RS8_HUMAN	0.84	0.03
60 S ribosomal protein L35a	RL35A_HUMAN	0.84	0.03
Histone H2A.V	H2AV_HUMAN	0.84	0.03
Splicing factor, proline- and glutamine-rich	SFPQ_HUMAN	0.84	0.03

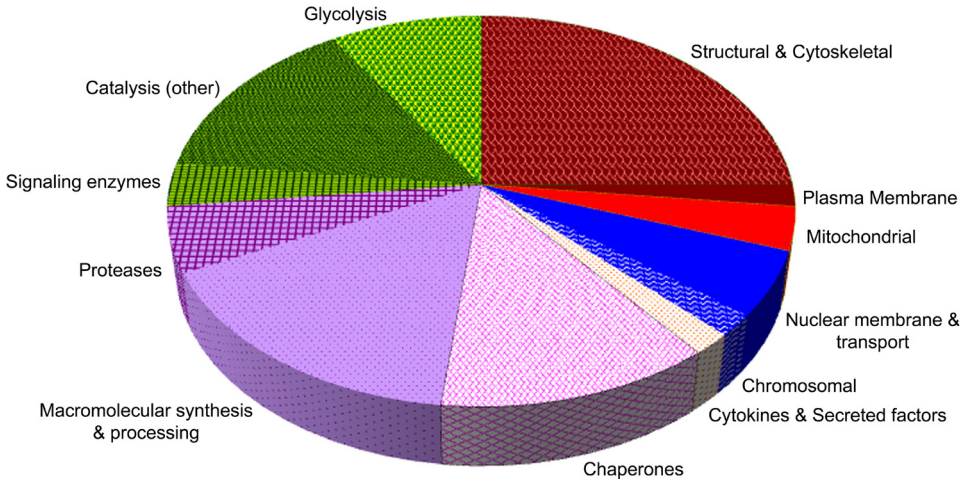

FIGURE 4. **Functional categorization of overrepresented proteins from apoptotic membrane vesicles.** Shown is the functional categorization (gene ontology) of proteins found to be enriched among apoptotic membrane vesicles by iTRAQ analysis (see Table 2). The two largest groups of proteins (26.8% each) are those characterized as membrane proteins and structural and cytoskeletal elements (shown in *brown*) and as catalytic proteins (shown in *green*). Proteins associated with the glycolytic pathway are the largest coherent cohort (9.0%) within either group. The next largest groups are proteins associated with macromolecular synthesis (especially translation) and processing and proteases (21.4%; shaded in *violet*) and molecular chaperones (12.5%; *cross-hatched magenta* area).

gous staining patterns were observed for the two other glycolytic enzymes that were analyzed, GAPDH (Fig. 6*B*) and TPI (Fig. 6*C*). Thus, glycolytic enzyme molecules not only are enriched among apoptotic membrane proteins but are exposed specifically on the apoptotic cell surface. Externalized glycolytic enzyme molecules fulfill the critical criteria for apoptotic determinants of recognition and immune modulation: they are evolutionarily conserved proteins that are resident in all cells ubiquitously and, although unexposed on the surface of viable cells, are membrane-exposed on apoptotic cells.

We evaluated the extent of glycolytic enzyme molecule externalization by comparing immunofluorescence staining of membrane-intact and permeabilized apoptotic cells. Examples of these analyses are presented in Fig. 7. Permeabilized viable and apoptotic cells stained identically and homogeneously for EnoA (Fig. 7*A*), GAPDH (Fig. 7*B*), and TPI (data not shown). The extent of externalization of these molecules ranged from 10 to 50% of the total cellular protein for each species during apoptotic cell death (by comparison of mean fluorescence intensities; see Fig. 7 legend). Importantly, these data indicate that the observed apoptosis-specific externalization of glycolytic enzyme molecules is distinct from a general accessibility to intracellular molecules that would result from plasma membrane compromise. In contrast, the detection of glycolytic enzyme molecules on necrotic cells is not distinguishable from plasma membrane compromise (see below). Our data also demonstrate that there is no net elevation of cellular glycolytic enzyme concentration with apoptosis, but rather a preferential externalization of those molecules.

We explored the kinetics of the appearance of these glycolytic enzyme molecules by examining the earliest apoptotic cells (annexin V^+/7-AAD^-) following brief treatment with

staurosporine, a potent inducer of apoptosis (Fig. 8). Externalized EnoA, GAPDH, and TPI could be found already externalized on these early apoptotic cells. Interestingly, the extent of exposure ranged as high as the levels found on later apoptotic cells. By comparison, neither autophagic or necrotic cells exposed glycolytic enzyme molecules (supplemental Fig. 1; note that we examined "early" (annexin V^+/7-AAD^-) necrotic cells (12) to preclude the detection of intracellular glycolytic molecules that become accessible with the loss of membrane integrity), consistent with the notion that the externalization of glycolytic enzyme molecules is a specific attribute of the apoptotic cell death process. Furthermore, we found that the process of glycolytic enzyme externalization, like apoptosis itself, is caspase-dependent (supplemental Fig. 2).

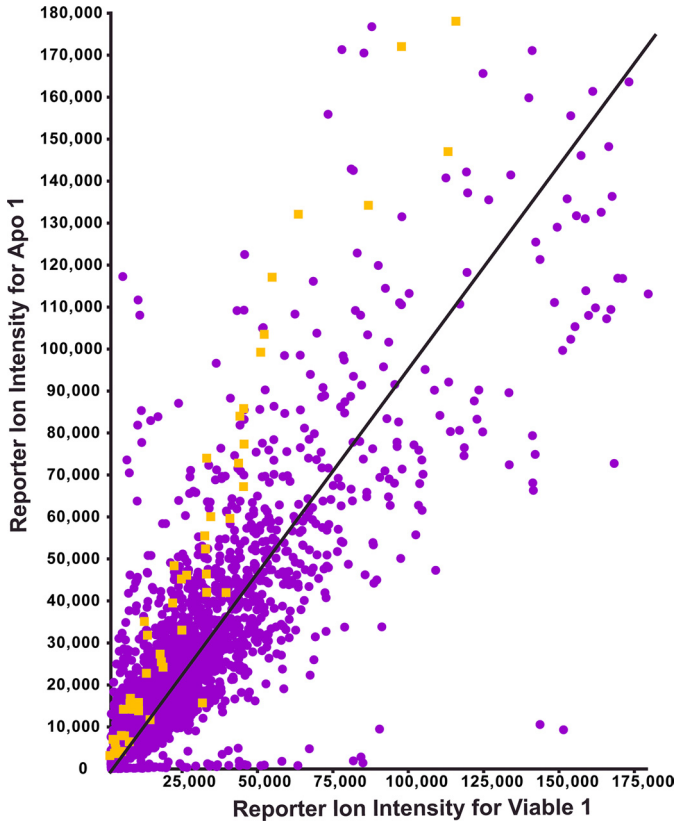

FIGURE 5. **Detail of EnoA data from iTRAQ analysis.** Shown is the overrepresentation of EnoA ascertained from the consistent iTRAQ ratios obtained from all related precursor ions. The plot shows reporter ion 114 (*Viable 1*) *versus* 116 (*Apo 1*) intensities for all peptides (*purple dots*) identified in iTRAQ experiment. *Yellow dots* represent the iTRAQ signals derived from spectra matched to EnoA (*Apo 1*).

These staining data involve a variety of mono- and polyclonal antibodies. Although all apoptotic cells reacted with polyclonal sera specific for the glycolytic enzymes, we noted differences among apoptotic cell populations with regard to reactivity with glycolytic enzyme-specific monoclonal antibodies (data not shown). Some glycolytic enzyme epitopes appear not to be exposed in some cell lines (although those epitopes are immunologically detectable intracellularly). These data suggest that the process of apoptosis-specific externalization may be constrained conformationally (see below).

In summary, our data from three independent approaches reveal that the externalization of glycolytic enzyme molecules is a dramatic event that occurs reliably and early during the process of apoptotic cell death. The surface-exposed, membrane-associated forms of glycolytic enzyme proteins represent novel and unambiguous apoptosis-specific biomarkers.

Externalized Glycolytic Enzyme Molecules Lack Enzymatic Activity—We assessed enolase and GAPDH activities in apoptotic and viable cells. Although apoptotic cells had elevated levels of apparently externalized activity, accounting for 40–50% of the total cellular activity observed in whole cell extracts (Table 4), virtually all of that externalized activity can be attributed to activity leaking from broken cells, *i.e.* we found equivalent activity in cell supernatants prepared by incubation of cells in reaction mixtures (that are of physiological osmolar-

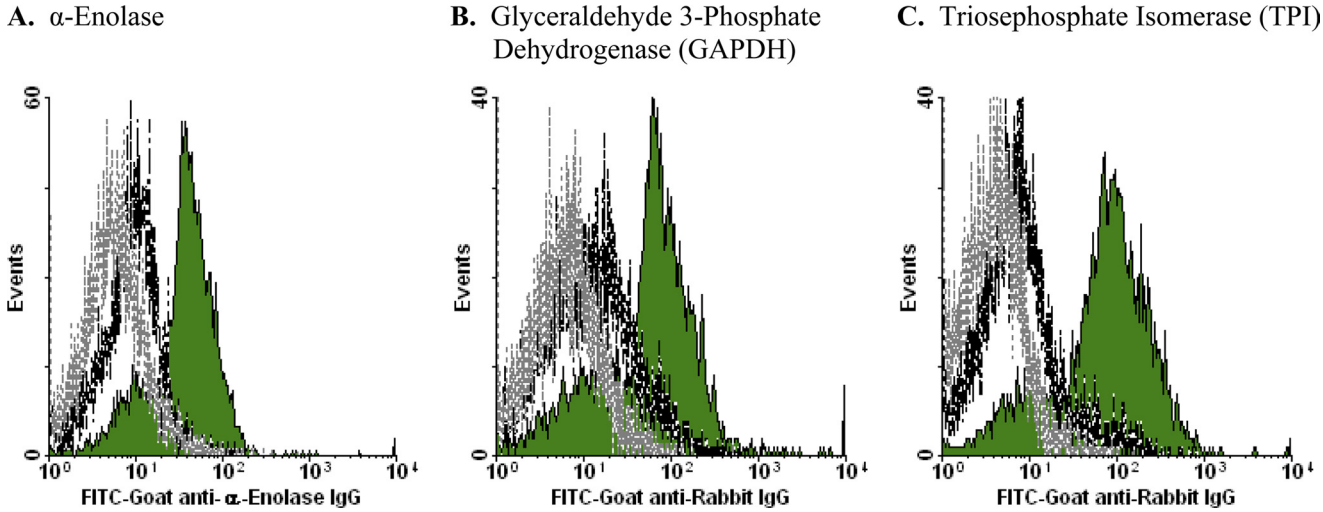

FIGURE 6. **Cytofluorometric analysis of externalization of glycolytic enzyme molecules.** Murine splenocytes that had undergone apoptosis spontaneously in culture (12 h) and freshly isolated, viable splenocytes were analyzed cytofluorometrically following staining with FITC-conjugated goat anti-EnoA peptide IgG polyclonal antibody (Santa Cruz Biotechnology) (*A*), rabbit anti-GAPDH IgG polyclonal antibody (Abcam) and FITC-conjugated goat anti-rabbit IgG secondary antibody (Santa Cruz Biotechnology) (*B*), and rabbit anti-TPI IgG polyclonal antibody (Novus Biologicals) and FITC-conjugated goat anti-rabbit IgG secondary antibody (*C*). Profiles shown are for apoptotic (*solid green* histograms) and viable (*black dashed lines*) cells stained with the specific FITC-conjugated reagents and for apoptotic cells stained with the secondary antibody alone (*gray dotted lines*). (The profile of viable cells is identical.) Cells that had lost membrane integrity (propidium iodide-positive, reduced forward- and expanded side-angle light scatter) were excluded from these analyses by electronic gating.

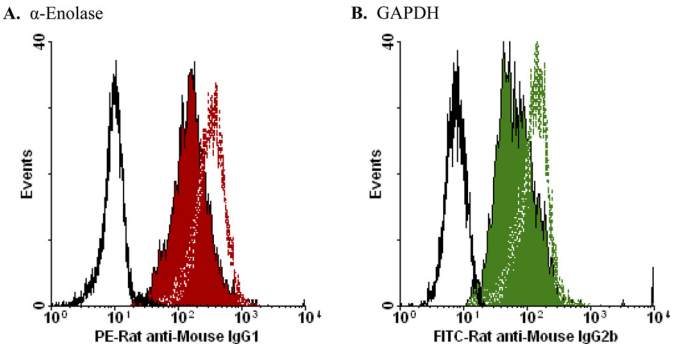

FIGURE 7. **Quantification of glycolytic enzyme molecule externalization.** Apoptotic cells (induced with actinomycin D) were analyzed cytofluorometrically without (*solid red* or *green* histogram) or following (*red* or *green dashed lines*) permeabilization. *A*, HeLa cells were stained with mouse anti-EnoA monoclonal antibody (L-27, Santa Cruz Biotechnology) and PE-conjugated rat anti-mouse IgG_1 secondary monoclonal antibody (BD Biosciences). The MFI of staining for non-permeabilized cells is 156.5; the MFI for permeabilized cells is 307.3; and the MFI for staining with secondary antibody alone (*black solid line*) is 10.0. We calculated the fraction of total cellular EnoA that was externalized in this experiment as 49%. The profile of staining of permeabilized viable HeLa cells (MFI = 319.5) was very similar to that of permeabilized apoptotic HeLa cells. *B*, DO11.10 cells were stained with mouse anti-GAPDH monoclonal antibody (Abcam) and FITC-conjugated rat anti-mouse IgG_{2b} secondary antibody (BD Biosciences). The MFI for non-permeabilized cells is 67.2; the MFI for permeabilized cells is 142.0; and the MFI for staining with secondary antibody alone (*black solid line*) is 15.2. The fraction of total cellular GAPDH externalized is 41%. The profile of staining of permeabilized viable DO11.10 cells (MFI = 138.5) was indistinguishable from that of permeabilized apoptotic DO11.10 cells.

ity) without substrate. Thus, we have no evidence that the "externalized" activities we observed represent the enzymatic activity of enzyme molecules localized to the cell surface as opposed to the activities of intracellular enzyme molecules released due to plasma membrane leakage. Indeed, we saw similar absolute levels of enolase and GAPDH activities associated with undisrupted cells from untreated cultures (although total cellular activities in apoptotic cultures were 40–60% lower than in viable cultures) (Table 4).

We conclude that apoptosis-specific externalized enzyme molecules are not enzymatically active. This conclusion is consistent with our suggestion that the process of apoptosis-specific externalization may be conformationally constrained (see above).

Externalized Glycolytic Enzyme Molecules Bind Plasminogen—Several of the glycolytic enzyme molecules that we have shown to be externalized with apoptosis (especially EnoA, GAPDH, and phosphoglycerate kinase) have been implicated previously in the binding of plasminogen (48–53). Elevated plasminogen binding associated with apoptotic cell death also has been described (54). Consistent with these observations, we observed robust plasminogen binding to apoptotic cells (Fig. 9*A*). Plasminogen binding, like glycolytic enzyme molecule externalization, was evident on the earliest apoptotic cells (Fig. 9*B*).

Pre-binding of plasminogen to apoptotic cells precluded the binding of EnoA-specific antibodies, indicating that EnoA serves as a plasminogen-binding "receptor" (data not shown), although it appears that EnoA is not the only species responsible for plasminogen binding to apoptotic cells. Conversely, plasminogen binding to the apoptotic cell surface was inhibited competitively with the lysine analog ϵ-aminocaproic acid (data not shown), consistent with the characterization of cell surface lysine residues as targets for plasminogen binding (48).

In contrast to the glycolytic enzyme molecules, annexin A2, which also has been implicated as a plasminogen-binding receptor (52), is not exposed preferentially during apoptotic cell death. There is concordance between iTRAQ and cytofluorometric analyses in this regard (Figs. 3 and 10*A*). By comparison, cytofluorometric analysis revealed the apoptosis-specific externalization of calreticulin (Fig. 10*B*), although our iTRAQ analysis did not identify calreticulin among apoptotic membrane vesicle-enriched molecules (Fig. 3). The exposure of calreticulin in association with apoptotic cell death has been noted previously (Ref. 55, but see Ref. 56).

DISCUSSION

Efficient recognition of the corpse, coupled to immunomodulation, is perhaps the ultimate functional consequence of apoptotic cell death, and the identification of the relevant molecules that determine those outcomes is of fundamental importance. On the basis of results from a variety of our studies indicating that apoptotic immunomodulatory determinants, which can be evaluated by the transcriptional responses they elicit, appear relatively early in the process of cell death, are enriched in plasma membrane vesicles from apoptotic cells, and are protease sensitive, we undertook distinct, independent, and unbiased proteomic approaches to characterize apoptosis-specific (compared with viable) membrane vesicle-associated proteins. We elaborated criteria that represent critical features of the molecules that function as apoptotic determinants for recognition and immune response modulation (denoted SUPER): molecules that become surface-exposed (during apoptotic cell death), ubiquitously expressed, protease-sensitive, evolutionarily conserved, and resident normally in viable cells (albeit not on the cell surface of non-apoptotic cells).

There were intriguing and informative surprises in the array of proteins identified. For example, the absence of histones, which meet the SUPER criteria for apoptotic determinants for recognition and immune modulation, is striking. The absence of histones from apoptotic vesicles may reflect their loose association with the apoptotic cell membrane and loss as a consequence of the extensive washing and ultracentrifugation involved in vesicle preparation. The apparent absence of actin (as distinct from molecules with which it shares significant sequence identity (*e.g.* actinin, etc.)) may simply represent an artifact of the informatic paradigm by which protein assignments from identified peptides are made, although, by immunofluorescence staining, we did not detect actin associated with apoptotic vesicles (data not shown). Presumably, the enrichment of cytochrome *c* among apoptotic vesicle proteins reflects the release of soluble cytochrome *c* from mitochondria during the apoptotic process, whereas the absence of cytochrome *c* from the cell surface underscores the selectivity of apoptosis-specific protein externalization.

Unexpectedly, we identified a group of glycolytic enzyme molecules that become redistributed and membrane-associated during apoptotic cell death, and we demonstrated cytofluorometrically their externalization to the apoptotic cell surface. With the exception of two of the upstream members

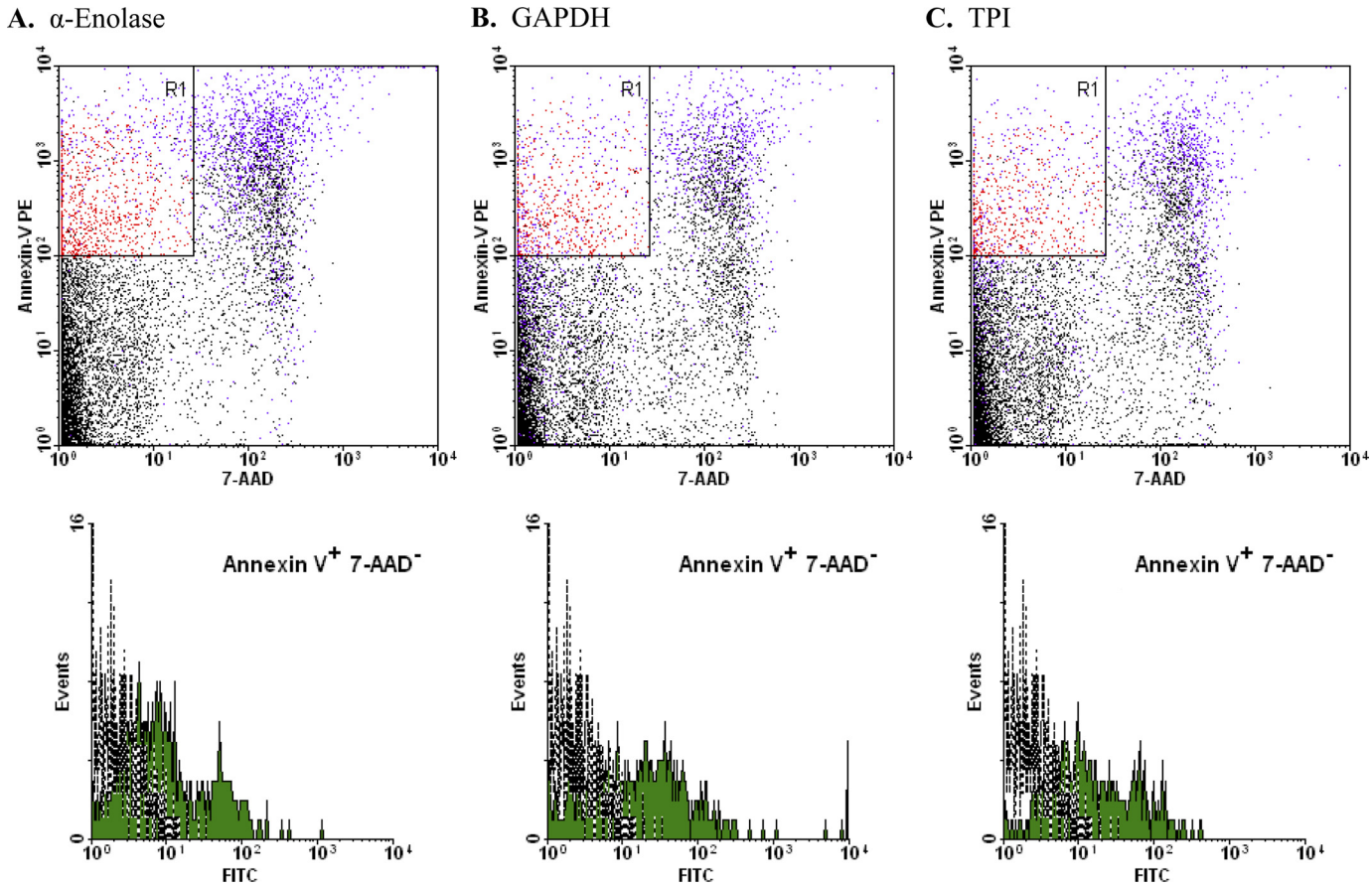

FIGURE 8. **Characterization of appearance of exposed glycolytic enzyme molecules.** Murine splenocytes that were induced to undergo apoptosis with staurosporine were analyzed cytofluorometrically following staining with PE-conjugated annexin V, 7-AAD, and FITC-conjugated goat anti-EnoA peptide IgG polyclonal antibody (*A*), rabbit anti-GAPDH IgG polyclonal antibody and FITC-conjugated goat anti-rabbit IgG secondary antibody (*B*), and rabbit anti-TPI IgG polyclonal antibody and FITC-conjugated goat anti-rabbit IgG secondary antibody (*C*). Cells that met the criteria of staining positively with annexin V and negatively with 7-AAD (*Annexin V$^+$ 7-AAD$^-$*; the *R1* region indicated in *red* in the *upper dot plots*) were gated electronically, and the fluorescein signal of those cells was analyzed (shown as *solid green* histograms in the *lower panels*). The fluorescein signal of annexin V$^+$/7-AAD$^-$ cells stained with secondary antibody alone also is presented (*gray dotted lines*).

TABLE 4

Cell-associated enzymatic activities

Enolase and GAPDH activities were assessed as described under "Experimental Procedures." Graded numbers of undisrupted viable or apoptotic HeLa cells or the sonicated extracts of equivalent cell numbers (disrupted cells) were incubated in 200-μl reactions for 4 min at 25 °C. Cells and cell debris were then removed by centrifugation, and reaction products were quantified spectrophotometrically. Activity in cell supernatants was assessed by incubating cells as described above in mock reactions without substrate, removing cells by centrifugation, and then incubating supernatants with substrate for an additional 4 min at 25 °C.

	Enolase activity (HeLa cells)[a]	
	Cells from viable populations	Cells from apoptotic populations
	nmol/10^4 cells	
Disrupted cell activity	9.7 ± 1.1	3.7 ± 0.8
Undisrupted cell activity	1.9 ± 0.4	1.9 ± 0.5
Undisrupted cell supernatant activity	1.4 ± 0.2	1.2 ± 0.2
	GAPDH activity (HeLa cells)[b]	
	Cells from viable populations	**Cells from apoptotic populations**
	nmol/10^4 cells	
Disrupted cell activity	5.5 ± 0.8	3.4 ± 0.1
Undisrupted cell activity	0.8 ± 0.1	1.4 ± 0.4
Undisrupted cell supernatant activity	1.2 ± 0.3	1.2 ± 0.1

[a] Conversion of 2-phosphoglycerate to phosphoenolpyruvate.
[b] Glyceraldehyde 3-phosphate-dependent formation of NADH.

(hexokinase and phosphofructokinase), all of the enzymes of the aerobic glycolytic pathway (phosphoglucose isomerase, aldolase, TPI, GAPDH, phosphoglycerate kinase, EnoA, and pyruvate kinase) were identified as enriched in the membrane vesicle fraction from apoptotic cells. Previous work (57, 58) has documented that glycolytic enzymes are not (normally) associated with the plasma membrane. Still, our results are consistent with findings from other proteomic studies. For example, Gu *et al.* (59) observed that several glycolytic enzymes (including EnoA and GAPDH) were up-regulated at late times of death (triggered by activation of p53), and Jin *et al.* (45) found EnoA and GAPDH in microparticles recovered from human plasma,

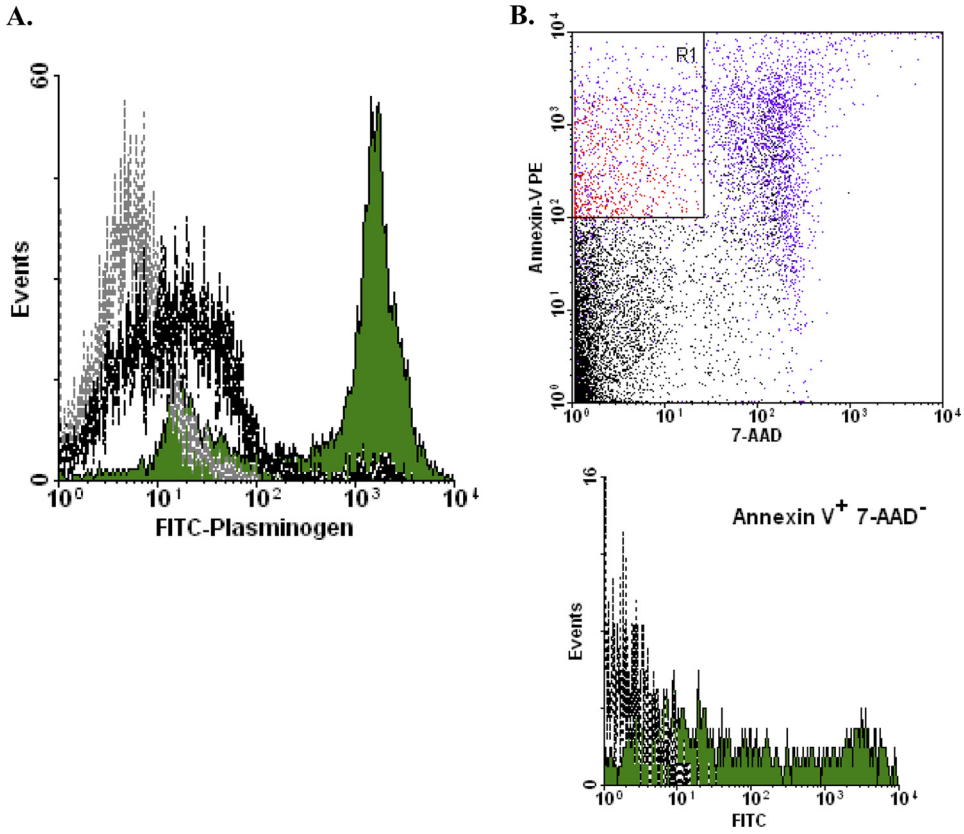

FIGURE 9. **Cytofluorometric analysis of plasminogen binding to apoptotic cells.** *A*, murine splenocytes that had undergone apoptosis spontaneously in culture (12 h) and freshly isolated, viable splenocytes were analyzed cytofluorometrically as described in the legend of Fig. 6 following staining with FITC-conjugated plasminogen. *B*, murine splenocytes that were induced to undergo apoptosis with staurosporine were analyzed cytofluorometrically following staining with PE-conjugated annexin V, 7-AAD, and FITC-conjugated plasminogen and analyzed as described in the legend of Fig. 8.

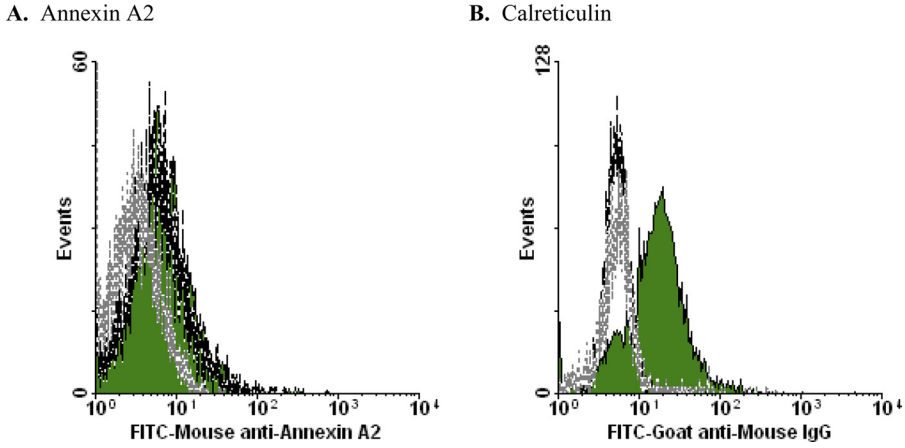

FIGURE 10. **Cytofluorometric analysis of externalization of other molecules.** Human transformed (Jurkat) T lymphocytes that had been induced to undergo apoptosis by treatment with actinomycin D or that had been left untreated were analyzed cytofluorometrically following staining with FITC-conjugated mouse anti-human annexin II monoclonal antibody (BD Biosciences) (*A*) or mouse anti-calreticulin monoclonal and FITC-conjugated goat anti-rabbit IgG secondary antibodies (Enzo Life Sciences) (*B*). Apoptotic (*solid green* histograms) and viable (*dashed lines*) cells were identified by scatter properties and gated electronically.

including apoptotic blebs. Sunaga *et al.* (60) also noted that GAPDH is overexpressed during the apoptotic death of neuronal cells and that it is exposed in amyloid plaques. Interestingly, these molecules have been shown to form multimeric complexes intracellularly on cytoskeletal and membrane elements in viable cells (61–64); we do not know if they exist in an aggregated form when externalized.

Our data demonstrate that glycolytic enzyme molecule externalization is a common and early aspect of apoptotic cell death in different cell types triggered to die with distinct suicidal stimuli. Although all apoptotic cells expose glycolytic enzyme molecules, only a fraction of those molecules within a cell are externalized to the cell surface; the externalized molecules lack enzymatic activity. Numerous metabolic processes and enzymes have been shown to be important for many aspects of apoptosis (65–68); however, the redistribution of a large subset of glycolytic enzymes to the apoptotic cell membrane has not been characterized previously. Our findings dem-

onstrate that the externalization of glycolytic enzyme molecules is a unique feature and a definitive marker of apoptotic cell death.

GAPDH and EnoA externalization has been noted previously in particular cases. For example, GAPDH has been reported to serve as a receptor for transferrin (30). Raje *et al.* (30) found that GAPDH was externalized on cells of a macrophage cell line cultured in iron-depleted medium. We repeated those experiments (with the same macrophage cell lines and others) and found that the iron-deficient conditions employed trigger apoptotic cell death, leading to the exposure of GAPDH (and other glycolytic enzyme molecules) (data not shown). Thus, these findings reiterate that externalized GAPDH is a definitive marker of the apoptotic cell, independent of transferrin-binding activity. The case of plasminogen binding to externalized EnoA is discussed below.

The cohort of externalized glycolytic enzyme molecules that we identified by several approaches fulfills the critical SUPER criteria. Others of the molecules enriched among apoptotic membrane vesicles and identified in our iTRAQ analysis also meet SUPER criteria. Those found not to be externalized (*e.g.* actin, cytochrome *c*, and histones; discussed above) likely can be excluded from further consideration. In addition, the group of chaperones likely does not function as apoptotic immunosuppressive determinants; heat shock proteins, in particular, have been implicated as immunostimulatory "danger signals" (69).

Furthermore, because exposure of resident intracellular molecules from necrotic cells does not confer apoptosis-like immunosuppressive activity (10, 12), protein externalization *per se* (in the absence of apoptosis-specific post-translational modification) likely is not sufficient for the appearance of apoptotic determinants for recognition and immune modulation. At least with regard to EnoA, our data demonstrating that the appearance of apoptotic determinants for recognition and immune response modulation is not dependent on *de novo* gene expression (10, 12) are consistent with the suggestion of Redlitz *et al.* (49) that the surface-exposed form of that molecule does not arise as the product of a specific or altered gene transcript.

It is not clear how apoptosis-specific protein externalization occurs, although our data indicate that it occurs in a caspase-dependent manner. The externalization of glycolytic enzymes has been observed in a wide variety of cells and among many species, independent of cell death (17–27, 48–50, 53). Among these examples are bacterial and protist pathogens, some of which have been shown to mimic apoptotic cell immune responses (70, 71). The export signals or mechanisms by which these normally intracellular molecules become membrane-exposed have not been identified. The enzymatically inactive forms of externalized glycolytic enzyme molecules on apoptotic cells contrast with the enzymatically active glycolytic enzymes exposed on the bacterial surface (17, 18, 20), suggesting that different processes for membrane externalization may pertain.

As discussed above, we observed similar mobilities (both relative molecular mass and pI) (Fig. 2) for non-externalized glycolytic enzyme molecules that are derived from viable cells and for the glycolytic enzyme molecules of apoptotic cells, at least a large fraction of which are externalized. With the exception of TPI, where there does appear to be apoptosis-enhanced proteolysis (Fig. 2, *spot 7′*), it is clear from these data that apoptosis-specific post-translational modifications that give rise to glycolytic enzyme molecule externalization generally are not proteolytic. Our analysis of such modifications, including the possibility of oxidation-dependent modification (72), is under way. Notably, apoptotic externalization appears to target proteins selectively and independently of protein abundance. The process of blebbing (73–76), which is characteristic of apoptosis, involves protein relocalization (1). We do not know whether blebbing *per se* is sufficient for the protein externalization that we have characterized.

Externalization of EnoA has been noted in the context of its ability to bind plasminogen (48–51). The nature of the cells exposing EnoA on the cell surface was not explored in those studies. Our data show that significant binding of plasminogen occurs specifically to apoptotic (and not viable) cells and that EnoA is involved in (at least some of) this binding. These results confirm and extend previous observations (54). In particular, independent studies have implicated externalized glycolytic enzymes (especially EnoA and GAPDH) on mammalian and pathogen surfaces as sites for plasminogen binding and activation (18, 27, 77, 78), although no compelling physiological rationale for the presence of this activity on such disparate cells has been offered.

Plasminogen binding, leading to proteolytic cleavage and plasmin activation, has been suggested to be important for pathogen invasiveness (27, 79). With mammalian cells, several (but not all) species of plasminogen receptor molecules are enriched on the surface of apoptotic cells. It seems unlikely that migration and invasiveness (*e.g.* extracellular matrix degradation) are selected attributes for apoptotic cells, although plasmin-dependent proteolytic activation of latent matrix-associated TGF-β may be significant (see Ref. 80). Plasminogen also appears to be a component of serum that enhances phagocytosis of apoptotic cells.[4] Although molecules identified as plasminogen receptors that are externalized in a non-cell death-related manner, such as annexin A2, may be physiologically relevant for plasminogen binding and its consequences (81, 82), plasminogen-binding molecules exposed in an apoptosis-specific manner may function in an entirely distinct capacity on the apoptotic cell surface.

Several molecular species of "plasminogen receptors" other than glycolytic enzyme molecules have been identified. For example, Plow and co-workers (83, 84) have suggested that histone H2B is a plasminogen receptor, and cell surface actin has been implicated similarly (44, 52, 85). In this context, it is interesting that our iTRAQ analysis indicated that these and other molecules characterized as (or associated with) plasminogen receptors (S100A10, annexin A2, and cytokeratin-8) (82, 86, 87) are not preferentially enriched on the apoptotic cell surface (Fig. 3).

We take our data to suggest that plasminogen binding *per se* may not represent the primary functional consequence of apoptosis-specific protein externalization; rather, the externaliza-

[4] K. Lauber, personal communication.

tion of glycolytic enzyme molecules may be significant functionally in apoptotic cell recognition and immune modulation. In this context, the significance of the expression of orthologous molecules on bacterial (and other pathogenic) surfaces may relate to apoptotic mimicry, leading to immune suppression (attenuation of inflammatory and other immune responses) rather than to plasminogen binding. Our results may then serve to integrate diverse previous findings to suggest that the observed binding of plasminogen to glycolytic enzyme molecules exposed on the mammalian cell surface is a consequence of the apoptosis-specific externalization of determinants for recognition and immune modulation and that apoptotic mimicry is the primary effect of exposed glycolytic molecules on commensal bacterial and pathogens.

Independently of their intracellular roles in metabolism (as well as more recently identified functions in transcription, cytoskeletal trafficking, and autophagy and cell death) (88–92), our findings proffer glycolytic enzyme molecules, in an extracellular context, as candidate determinants of immunomodulation and suggest that they may fulfill an immunological "moonlighting" (93) role. It is not surprising that, in cases of autoimmune pathology, where normal innate apoptotic immunity and tolerance are broken, these molecules are recognized as autoantigens to which antibodies are generated. Indeed, glycolytic enzymes have been identified as potent autoantigens in several autoimmune syndromes, *e.g.* EnoA in Hashimoto encephalopathy, Behçet disease, systemic lupus erythematosus, inflammatory bowel disease, vasculitis, mixed cryoglobulinemia, and rheumatoid arthritis (94–100); TPI in neuropsychiatric lupus, systemic lupus erythematosus, and osteoarthritis (101, 102); and pyruvate kinase in rheumatoid arthritis and systemic lupus erythematosus (103). Further characterization of the apoptosis-specific mechanism by which glycolytic enzymes are post-translationally modified and externalized and their role in immune modulation holds promise for understanding and addressing causes of autoimmune and inflammatory pathology.

Acknowledgments—D. S. U. gratefully acknowledges Michael Federle and Nancy Freitag for recognizing a parallel between apoptotic and bacterial glycolytic enzyme externalization.

REFERENCES

1. Cocca, B. A., Cline, A. M., and Radic, M. Z. (2002) Blebs and apoptotic bodies are B cell autoantigens. *J. Immunol.* **169,** 159–166
2. Kerr, J. F., Wyllie, A. H., and Currie, A. R. (1972) Apoptosis: a basic biological phenomenon with wide-ranging implications in tissue kinetics. *Br. J. Cancer* **26,** 239–257
3. Savill, J., Dransfield, I., Gregory, C., and Haslett, C. (2002) A blast from the past: clearance of apoptotic cells regulates immune responses. *Nat. Rev. Immunol.* **2,** 965–975
4. Birge, R. B., and Ucker, D. S. (2008) Innate apoptotic immunity: the calming touch of death. *Cell Death Differ.* **15,** 1096–1102
5. Herrmann, M., Voll, R. E., Zoller, O. M., Hagenhofer, M., Ponner, B. B., and Kalden, J. R. (1998) Impaired phagocytosis of apoptotic cell material by monocyte-derived macrophages from patients with systemic lupus erythematosus. *Arthritis Rheum.* **41,** 1241–1250
6. Cohen, P. L., Caricchio, R., Abraham, V., Camenisch, T. D., Jennette, J. C., Roubey, R. A., Earp, H. S., Matsushima, G., and Reap, E. A. (2002) Delayed apoptotic cell clearance and lupus-like autoimmunity in mice lacking the c-mer membrane tyrosine kinase. *J. Exp. Med.* **196,** 135–140
7. Rothlin, C. V., Ghosh, S., Zuniga, E. I., Oldstone, M. B., and Lemke, G. (2007) TAM receptors are pleiotropic inhibitors of the innate immune response. *Cell* **131,** 1124–1136
8. Thorp, E. B. (2010) Mechanisms of failed apoptotic cell clearance by phagocyte subsets in cardiovascular disease. *Apoptosis* **15,** 1124–1136
9. Ucker, D. S. (2009) in *Phagocytosis of Dying Cells: From Molecular Mechanisms to Human Diseases* (Krysko, D. V., and Vandenabeele, P., eds), pp. 163–187 Springer, New York
10. Cvetanovic, M., and Ucker, D. S. (2004) Innate immune discrimination of apoptotic cells: repression of proinflammatory macrophage transcription is coupled directly to specific recognition. *J. Immunol.* **172,** 880–889
11. Patel, V. A., Longacre-Antoni, A., Cvetanovic, M., Lee, D. J., Feng, L., Fan, H., Rauch, J., Ucker, D. S., and Levine, J. S. (2007) The affirmative response of the innate immune system to apoptotic cells. *Autoimmunity* **40,** 274–280
12. Cocco, R. E., and Ucker, D. S. (2001) Distinct modes of macrophage recognition for apoptotic and necrotic cells are not specified exclusively by phosphatidylserine exposure. *Mol. Biol. Cell* **12,** 919–930
13. Cvetanovic, M., Mitchell, J. E., Patel, V., Avner, B. S., Su, Y., van der Saag, P. T., Witte, P. L., Fiore, S., Levine, J. S., and Ucker, D. S. (2006) Specific recognition of apoptotic cells reveals a ubiquitous and unconventional innate immunity. *J. Biol. Chem.* **281,** 20055–20067
14. Fadok, V. A., Bratton, D. L., Konowal, A., Freed, P. W., Westcott, J. Y., and Henson, P. M. (1998) Macrophages that have ingested apoptotic cells *in vitro* inhibit proinflammatory cytokine production through autocrine/paracrine mechanisms involving TGF-β, PGE_2, and PAF. *J. Clin. Invest.* **101,** 890–898
15. Savill, J. (1998) Apoptosis. Phagocytic docking without shocking. *Nature* **392,** 442–443
16. Fadok, V. A., Voelker, D. R., Campbell, P. A., Cohen, J. J., Bratton, D. L., and Henson, P. M. (1992) Exposure of phosphatidylserine on the surface of apoptotic lymphocytes triggers specific recognition and removal by macrophages. *J. Immunol.* **148,** 2207–2216
17. Pancholi, V., and Fischetti, V. A. (1992) A major surface protein on group A streptococci is a glyceraldehyde-3-phosphate dehydrogenase with multiple binding activity. *J. Exp. Med.* **176,** 415–426
18. Bergmann, S., Rohde, M., Chhatwal, G. S., and Hammerschmidt, S. (2001) α-Enolase of *Streptococcus pneumoniae* is a plasmin(ogen)-binding protein displayed on the bacterial cell surface. *Mol. Microbiol.* **40,** 1273–1287
19. Bergmann, S., Rohde, M., and Hammerschmidt, S. (2004) Glyceraldehyde-3-phosphate dehydrogenase of *Streptococcus pneumoniae* is a surface-displayed plasminogen-binding protein. *Infect. Immun.* **72,** 2416–2419
20. Pancholi, V., and Fischetti, V. A. (1998) α-Enolase, a novel strong plasmin(ogen) binding protein on the surface of pathogenic streptococci. *J. Biol. Chem.* **273,** 14503–14515
21. Candela, M., Biagi, E., Centanni, M., Turroni, S., Vici, M., Musiani, F., Vitali, B., Bergmann, S., Hammerschmidt, S., and Brigidi, P. (2009) Bifidobacterial enolase, a cell surface receptor for human plasminogen involved in the interaction with the host. *Microbiology* **155,** 3294–3303
22. Vanegas, G., Quiñones, W., Carrasco-López, C., Concepción, J. L., Albericio, F., and Avilán, L. (2007) Enolase as a plasminogen-binding protein in *Leishmania mexicana*. *Parasitol. Res.* **101,** 1511–1516
23. Lama, A., Kucknoor, A., Mundodi, V., and Alderete, J. F. (2009) Glyceraldehyde-3-phosphate dehydrogenase is a surface-associated, fibronectin-binding protein of *Trichomonas vaginalis*. *Infect. Immun.* **77,** 2703–2711
24. Bhowmick, I. P., Kumar, N., Sharma, S., Coppens, I., and Jarori, G. K. (2009) *Plasmodium falciparum* enolase: stage-specific expression and subcellular localization. *Malar. J.* **8,** 179
25. Gil-Navarro, I., Gil, M. L., Casanova, M., O'Connor, J. E., Martínez, J. P., and Gozalbo, D. (1997) The glycolytic enzyme glyceraldehyde-3-phosphate dehydrogenase of *Candida albicans* is a surface antigen. *J. Bacte-*

riol. **179,** 4992–4999
26. Goudot-Crozel, V., Caillol, D., Djabali, M., and Dessein, A. J. (1989) The major parasite surface antigen associated with human resistance to schistosomiasis is a 37-kDa glyceraldehyde-3-phosphate dehydrogenase. *J. Exp. Med.* **170,** 2065–2080
27. Jong, A. Y., Chen, S. H., Stins, M. F., Kim, K. S., Tuan, T. L., and Huang, S. H. (2003) Binding of *Candida albicans* enolase to plasmin(ogen) results in enhanced invasion of human brain microvascular endothelial cells. *J. Med. Microbiol.* **52,** 615–622
28. Chang, S. H., Cvetanovic, M., Harvey, K. J., Komoriya, A., Packard, B. Z., and Ucker, D. S. (2002) The effector phase of physiological cell death relies exclusively on the post-translational activation of resident components. *Exp. Cell Res.* **277,** 15–30
29. Kabeya, Y., Mizushima, N., Ueno, T., Yamamoto, A., Kirisako, T., Noda, T., Kominami, E., Ohsumi, Y., and Yoshimori, T. (2000) LC3, a mammalian homolog of yeast Apg8p, is localized in autophagosome membranes after processing. *EMBO J.* **19,** 5720–5828
30. Raje, C. I., Kumar, S., Harle, A., Nanda, J. S., and Raje, M. (2007) The macrophage cell surface glyceraldehyde-3-phosphate dehydrogenase is a novel transferrin receptor. *J. Biol. Chem.* **282,** 3252–3261
31. Rouser, G., Fleischer, S., and Yamamoto, A. (1970) Two-dimensional thin layer chromatographic separation of polar lipids and determination of phospholipids by phosphorus analysis of spots. *Lipids* **5,** 494–496
32. Jain, M. R., Bian, S., Liu, T., Hu, J., Elkabes, S., and Li, H. (2009) Altered proteolytic events in experimental autoimmune encephalomyelitis discovered by iTRAQ shotgun proteomics analysis of spinal cord. *Proteome Sci.* **7,** 25
33. Jain, M. R., Liu, T., Hu, J., Darfler, M., Fitzhugh, V., Rinaggio, J., and Li, H. (2008) Quantitative proteomic analysis of formalin-fixed paraffin-embedded oral HPV lesions from HIV patients. *Open Proteomics J.* **1,** 40–45
34. Keller, A., Nesvizhskii, A. I., Kolker, E., and Aebersold, R. (2002) Empirical statistical model to estimate the accuracy of peptide identifications made by MS/MS and database search. *Anal. Chem.* **74,** 5383–5392
35. Nesvizhskii, A. I., Keller, A., Kolker, E., and Aebersold, R. (2003) A statistical model for identifying proteins by tandem mass spectrometry. *Anal. Chem.* **75,** 4646–4658
36. Kanapka, J. A., and Hamilton, I. R. (1971) Fluoride inhibition of enolase activity *in vivo* and its relationship to the inhibition of glucose-6-P formation in *Streptococcus salivarius*. *Arch. Biochem. Biophys.* **146,** 167–174
37. Mannherz, H. G., Gonsior, S. M., Gremm, D., Wu, X., Pope, B. J., and Weeds, A. G. (2005) Activated cofilin colocalizes with Arp2/3 complex in apoptotic blebs during programmed cell death. *Eur. J. Cell Biol.* **84,** 503–515
38. Buttyan, R., Zakeri, Z., Lockshin, R., and Wolgemuth, D. (1988) Cascade induction of c-*fos*, c-*myc*, and heat shock 70K transcripts during regression of the rat ventral prostate gland. *Mol. Endocrinol.* **2,** 650–657
39. Zinszner, H., Kuroda, M., Wang, X., Batchvarova, N., Lightfoot, R. T., Remotti, H., Stevens, J. L., and Ron, D. (1998) CHOP is implicated in programmed cell death in response to impaired function of the endoplasmic reticulum. *Genes Dev.* **12,** 982–995
40. Huot, J., Houle, F., Rousseau, S., Deschesnes, R. G., Shah, G. M., and Landry, J. (1998) SAPK2/p38-dependent F-actin reorganization regulates early membrane blebbing during stress-induced apoptosis. *J. Cell Biol.* **143,** 1361–1373
41. Kluck, R. M., Bossy-Wetzel, E., Green, D. R., and Newmeyer, D. D. (1997) The release of cytochrome *c* from mitochondria: a primary site for Bcl-2 regulation of apoptosis. *Science* **275,** 1132–1136
42. D'Herde, K., De Prest, B., Mussche, S., Schotte, P., Beyaert, R., Van Coster, R., and Roels, F. (2000) Ultrastructural localization of cytochrome *c* in apoptosis demonstrates mitochondrial heterogeneity. *Cell Death Differ.* **7,** 331–337
43. Laster, S. M., and Mackenzie, J. M., Jr. (1996) Bleb formation and F-actin distribution during mitosis and tumor necrosis factor-induced apoptosis. *Microsc. Res. Tech.* **34,** 272–280
44. Dudani, A. K., and Ganz, P. R. (1996) Endothelial cell surface actin serves as a binding site for plasminogen, tissue plasminogen activator, and lipoprotein(a). *Br. J. Haematol.* **95,** 168–178
45. Jin, M., Drwal, G., Bourgeois, T., Saltz, J., and Wu, H. M. (2005) Distinct proteome features of plasma microparticles. *Proteomics* **5,** 1940–1952
46. Arur, S., Uche, U. E., Rezaul, K., Fong, M., Scranton, V., Cowan, A. E., Mohler, W., and Han, D. K. (2003) Annexin I is an endogenous ligand that mediates apoptotic cell engulfment. *Dev. Cell* **4,** 587–598
47. Miguet, L., Pacaud, K., Felden, C., Hugel, B., Martinez, M. C., Freyssinet, J. M., Herbrecht, R., Potier, N., van Dorsselaer, A., and Mauvieux, L. (2006) Proteomic analysis of malignant lymphocyte membrane microparticles using double ionization coverage optimization. *Proteomics* **6,** 153–171
48. Miles, L. A., Dahlberg, C. M., Plescia, J., Felez, J., Kato, K., and Plow, E. F. (1991) Role of cell surface lysines in plasminogen binding to cells: identification of α-enolase as a candidate plasminogen receptor. *Biochemistry* **30,** 1682–1691
49. Redlitz, A., Fowler, B. J., Plow, E. F., and Miles, L. A. (1995) The role of an enolase-related molecule in plasminogen binding to cells. *Eur. J. Biochem.* **227,** 407–415
50. Nakajima, K., Hamanoue, M., Takemoto, N., Hattori, T., Kato, K., and Kohsaka, S. (1994) Plasminogen binds specifically to α-enolase on rat neuronal plasma membrane. *J. Neurochem.* **63,** 2048–2057
51. López-Alemany, R., Suelves, M., and Muñoz-Cánoves, P. (2003) Plasmin generation dependent on α-enolase-type plasminogen receptor is required for myogenesis. *Thromb. Haemost.* **90,** 724–733
52. Kwon, M., MacLeod, T. J., Zhang, Y., and Waisman, D. M. (2005) S100A10, annexin A2, and annexin A2 heterotetramer as candidate plasminogen receptors. *Front. Biosci.* **10,** 300–325
53. Wygrecka, M., Marsh, L. M., Morty, R. E., Henneke, I., Guenther, A., Lohmeyer, J., Markart, P., and Preissner, K. T. (2009) Enolase-1 promotes plasminogen-mediated recruitment of monocytes to the acutely inflamed lung. *Blood* **113,** 5588–5598
54. O'Mullane, M. J., and Baker, M. S. (1998) Loss of cell viability dramatically elevates cell surface plasminogen binding and activation. *Exp. Cell Res.* **242,** 153–164
55. Obeid, M., Tesniere, A., Ghiringhelli, F., Fimia, G. M., Apetoh, L., Perfettini, J. L., Castedo, M., Mignot, G., Panaretakis, T., Casares, N., Métivier, D., Larochette, N., van Endert, P., Ciccosanti, F., Piacentini, M., Zitvogel, L., and Kroemer, G. (2007) Calreticulin exposure dictates the immunogenicity of cancer cell death. *Nat. Med.* **13,** 54–61
56. Gardai, S. J., McPhillips, K. A., Frasch, S. C., Janssen, W. J., Starefeldt, A., Murphy-Ullrich, J. E., Bratton, D. L., Oldenborg, P. A., Michalak, M., and Henson, P. M. (2005) Cell surface calreticulin initiates clearance of viable or apoptotic cells through transactivation of LRP on the phagocyte. *Cell* **123,** 321–334
57. Shui, W., Sheu, L., Liu, J., Smart, B., Petzold, C. J., Hsieh, T. Y., Pitcher, A., Keasling, J. D., and Bertozzi, C. R. (2008) Membrane proteomics of phagosomes suggests a connection to autophagy. *Proc. Natl. Acad. Sci. U.S.A.* **105,** 16952–16957
58. Rogers, L. D., and Foster, L. J. (2007) The dynamic phagosomal proteome and the contribution of the endoplasmic reticulum. *Proc. Natl. Acad. Sci. U.S.A.* **104,** 18520–18525
59. Gu, S., Liu, Z., Pan, S., Jiang, Z., Lu, H., Amit, O., Bradbury, E. M., Hu, C. A., and Chen, X. (2004) Global investigation of p53-induced apoptosis through quantitative proteomic profiling using comparative amino acid-coded tagging. *Mol. Cell. Proteomics* **3,** 998–1008
60. Sunaga, K., Takahashi, H., Chuang, D. M., and Ishitani, R. (1995) Glyceraldehyde-3-phosphate dehydrogenase is overexpressed during apoptotic death of neuronal cultures and is recognized by a monoclonal antibody against amyloid plaques from Alzheimer brain. *Neurosci. Lett.* **200,** 133–136
61. Srere, P. A., and Knull, H. R. (1998) Location-location-location. *Trends Biochem. Sci.* **23,** 319–320
62. Singh, P., Salih, M., Leddy, J. J., and Tuana, B. S. (2004) The muscle-specific calmodulin-dependent protein kinase assembles with the glycolytic enzyme complex at the sarcoplasmic reticulum and modulates the activity of glyceraldehyde-3-phosphate dehydrogenase in a Ca^{2+}/calmodulin-dependent manner. *J. Biol. Chem.* **279,** 35176–35182
63. Minaschek, G., Gröschel-Stewart, U., Blum, S., and Bereiter-Hahn, J.

(1992) Microcompartmentation of glycolytic enzymes in cultured cells. *Eur. J. Cell Biol.* **58,** 418–428
64. Campanella, M. E., Chu, H., and Low, P. S. (2005) Assembly and regulation of a glycolytic enzyme complex on the human erythrocyte membrane. *Proc. Natl. Acad. Sci. U.S.A.* **102,** 2402–2407
65. Ishitani, R., and Chuang, D. M. (1996) Glyceraldehyde-3-phosphate dehydrogenase antisense oligodeoxynucleotides protect against cytosine arabinonucleoside-induced apoptosis in cultured cerebellar neurons. *Proc. Natl. Acad. Sci. U.S.A.* **93,** 9937–9941
66. Eguchi, Y., Shimizu, S., and Tsujimoto, Y. (1997) Intracellular ATP levels determine cell death fate by apoptosis or necrosis. *Cancer Res.* **57,** 1835–1840
67. Leist, M., Single, B., Castoldi, A. F., Kühnle, S., and Nicotera, P. (1997) Intracellular adenosine triphosphate (ATP) concentration: a switch in the decision between apoptosis and necrosis. *J. Exp. Med.* **185,** 1481–1486
68. Robey, R. B., and Hay, N. (2006) Mitochondrial hexokinases, novel mediators of the anti-apoptotic effects of growth factors and Akt. *Oncogene* **25,** 4683–4696
69. Manjili, M. H., Park, J., Facciponte, J. G., and Subjeck, J. R. (2005) HSP110 induces "danger signals" upon interaction with antigen-presenting cells and mouse mammary carcinoma. *Immunobiology* **210,** 295–303
70. de Freitas Balanco, J. M., Moreira, M. E., Bonomo, A., Bozza, P. T., Amarante-Mendes, G., Pirmez, C., and Barcinski, M. A. (2001) Apoptotic mimicry by an obligate intracellular parasite down-regulates macrophage microbicidal activity. *Curr. Biol.* **11,** 1870–1873
71. Barcinski, M. A., Moreira, M. E., de Freitas Balanco, J. M., Wanderley, J. L., and Bonomo, A. C. (2003) The role of apoptotic mimicry in host-parasite interplay: is death the only alternative for altruistic behavior? *Kinetoplastid Biol. Dis.* **2,** 6–7
72. Sambrano, G. R., and Steinberg, D. (1995) Recognition of oxidatively damaged and apoptotic cells by an oxidized low density lipoprotein receptor on mouse peritoneal macrophages: role of membrane phosphatidylserine. *Proc. Natl. Acad. Sci. U.S.A.* **92,** 1396–1400
73. Mills, J. C., Stone, N. L., Erhardt, J., and Pittman, R. N. (1998) Apoptotic membrane blebbing is regulated by myosin light chain phosphorylation. *J. Cell Biol.* **140,** 627–636
74. Coleman, M. L., Sahai, E. A., Yeo, M., Bosch, M., Dewar, A., and Olson, M. F. (2001) Membrane blebbing during apoptosis results from caspase-mediated activation of ROCK I. *Nat. Cell Biol.* **3,** 339–345
75. Sebbagh, M., Renvoizé, C., Hamelin, J., Riché, N., Bertoglio, J., and Bréard, J. (2001) Caspase-3-mediated cleavage of ROCK I induces MLC phosphorylation and apoptotic membrane blebbing. *Nat. Cell Biol.* **3,** 346–352
76. Leverrier, Y., and Ridley, A. J. (2001) Apoptosis: caspases orchestrate the ROCK "n" bleb. *Nat. Cell Biol.* **3,** E91–E93
77. Felez, J., Chanquia, C. J., Fabregas, P., Plow, E. F., and Miles, L. A. (1993) Competition between plasminogen and tissue plasminogen activator for cellular binding sites. *Blood* **82,** 2433–2441
78. Miles, L. A., Hawley, S. B., Baik, N., Andronicos, N. M., Castellino, F. J., and Parmer, R. J. (2005) Plasminogen receptors: the *sine qua non* of cell surface plasminogen activation. *Front. Biosci.* **10,** 1754–1762
79. Lähteenmäki, K., Edelman, S., and Korhonen, T. K. (2005) Bacterial metastasis: the host plasminogen system in bacterial invasion. *Trends Microbiol.* **13,** 79–85
80. Plow, E. F., Herren, T., Redlitz, A., Miles, L. A., and Hoover-Plow, J. L. (1995) The cell biology of the plasminogen system. *FASEB J.* **9,** 939–945
81. Odaka, C., Tanioka, M., and Itoh, T. (2005) Matrix metalloproteinase-9 in macrophages induces thymic neovascularization following thymocyte apoptosis. *J. Immunol.* **174,** 846–853
82. Falcone, D. J., Borth, W., Khan, K. M., and Hajjar, K. A. (2001) Plasminogen-mediated matrix invasion and degradation by macrophages is dependent on surface expression of annexin II. *Blood* **97,** 777–784
83. Das, R., Burke, T., and Plow, E. F. (2007) Histone H2B as a functionally important plasminogen receptor on macrophages. *Blood* **110,** 3763–3772
84. Herren, T., Burke, T. A., Das, R., and Plow, E. F. (2006) Identification of histone H2B as a regulated plasminogen receptor. *Biochemistry* **45,** 9463–9474
85. Hawley, S. B., Green, M. A., and Miles, L. A. (2000) Discriminating between cell surface and intracellular plasminogen-binding proteins: heterogeneity in profibrinolytic plasminogen-binding proteins on monocytoid cells. *Thromb. Haemost.* **84,** 882–890
86. Ling, Q., Jacovina, A. T., Deora, A., Febbraio, M., Simantov, R., Silverstein, R. L., Hempstead, B., Mark, W. H., and Hajjar, K. A. (2004) Annexin II regulates fibrin homeostasis and neoangiogenesis *in vivo*. *J. Clin. Invest.* **113,** 38–48
87. Cesarman, G. M., Guevara, C. A., and Hajjar, K. A. (1994) An endothelial cell receptor for plasminogen/tissue plasminogen activator (t-PA). II. Annexin II-mediated enhancement of t-PA-dependent plasminogen activation. *J. Biol. Chem.* **269,** 21198–22203
88. Feo, S., Arcuri, D., Piddini, E., Passantino, R., and Giallongo, A. (2000) ENO1 gene product binds to the c-*myc* promoter and acts as a transcriptional repressor: relationship with Myc promoter-binding protein 1 (MBP-1). *FEBS Lett.* **473,** 47–52
89. Colell, A., Ricci, J. E., Tait, S., Milasta, S., Maurer, U., Bouchier-Hayes, L., Fitzgerald, P., Guio-Carrion, A., Waterhouse, N. J., Li, C. W., Mari, B., Barbry, P., Newmeyer, D. D., Beere, H. M., and Green, D. R. (2007) GAPDH and autophagy preserve survival after apoptotic cytochrome *c* release in the absence of caspase activation. *Cell* **129,** 983–997
90. Tisdale, E. J. (2002) Glyceraldehyde-3-phosphate dehydrogenase is phosphorylated by protein kinase Cι/λ and plays a role in microtubule dynamics in the early secretory pathway. *J. Biol. Chem.* **277,** 3334–3341
91. Glaser, P. E., Han, X., and Gross, R. W. (2002) Tubulin is the endogenous inhibitor of the glyceraldehyde-3-phosphate dehydrogenase isoform that catalyzes membrane fusion: implications for the coordinated regulation of glycolysis and membrane fusion. *Proc. Natl. Acad. Sci. U.S.A.* **99,** 14104–14109
92. Tisdale, E. J., Azizi, F., and Artalejo, C. R. (2009) Rab2 utilizes glyceraldehyde-3-phosphate dehydrogenase and protein kinase Cι to associate with microtubules and to recruit dynein. *J. Biol. Chem.* **284,** 5876–5884
93. Jeffery, C. J. (2009) Moonlighting proteins–an update. *Mol. BioSyst.* **5,** 345–350
94. Sabbatini, A., Dolcher, M. P., Marchini, B., Chimenti, D., Moscato, S., Pratesi, F., Bombardieri, S., and Migliorini, P. (1997) α-Enolase is a renal-specific antigen associated with kidney involvement in mixed cryoglobulinemia. *Clin. Exp. Rheumatol.* **15,** 655–658
95. Roozendaal, C., Zhao, M. H., Horst, G., Lockwood, C. M., Kleibeuker, J. H., Limburg, P. C., Nelis, G. F., and Kallenberg, C. G.(1998) Catalase and α-enolase: two novel granulocyte autoantigens in inflammatory bowel disease (IBD). *Clin. Exp. Immunol.* **112,** 10–16
96. Pratesi, F., Moscato, S., Sabbatini, A., Chimenti, D., Bombardieri, S., and Migliorini, P. (2000) Autoantibodies specific for α-enolase in systemic autoimmune disorders. *J. Rheumatol.* **27,** 109–115
97. Moscato, S., Pratesi, F., Sabbatini, A., Chimenti, D., Scavuzzo, M., Passatino, R., Bombardieri, S., Giallongo, A., and Migliorini, P. (2000) Surface expression of a glycolytic enzyme, α-enolase, recognized by autoantibodies in connective tissue disorders. *Eur. J. Immunol.* **30,** 3575–3584
98. Saulot, V., Vittecoq, O., Charlionet, R., Fardellone, P., Lange, C., Marvin, L., Machour, N., Le Loët, X., Gilbert, D., and Tron, F. (2002) Presence of autoantibodies to the glycolytic enzyme α-enolase in sera from patients with early rheumatoid arthritis. *Arthritis Rheum.* **46,** 1196–1201
99. Lee, K. H., Chung, H. S., Kim, H. S., Oh, S. H., Ha, M. K., Baik, J. H., Lee, S., and Bang, D. (2003) Human α-enolase from endothelial cells as a target antigen of anti-endothelial cell antibody in Behçet disease. *Arthritis Rheum.* **48,** 2025–2035
100. Fujii, A., Yoneda, M., Ito, T., Yamamura, O., Satomi, S., Higa, H., Kimura, A., Suzuki, M., Yamashita, M., Yuasa, T., Suzuki, H., and Kuriyama, M. (2005) Autoantibodies against the amino terminal of α-enolase are a useful diagnostic marker of Hashimoto encephalopathy. *J. Neuroimmunol.* **162,** 130–136
101. Xiang, Y., Sekine, T., Nakamura, H., Imajoh-Ohmi, S., Fukuda, H., Nishioka, K., and Kato, T. (2004) Proteomic surveillance of autoimmunity in osteoarthritis: identification of triose-phosphate isomerase as an autoantigen in patients with osteoarthritis. *Arthritis Rheum.* **50,** 1511–1521
102. Sasajima, T., Watanabe, H., Sato, S., Sato, Y., and Ohira, H. (2006) Anti-triose-phosphate isomerase antibodies in cerebrospinal fluid are associ-

ated with neuropsychiatric lupus. *J. Neuroimmunol.* **181,** 150–156
103. Oremek, G. M., Müller, R., Sapoutzis, N., and Wigand, R. (2003) Pyruvate kinase-type tumor M2 plasma levels in patients afflicted with rheumatic diseases. *Anticancer Res.* **23,** 1131–1134
104. Kato, H., Fukuda, T., Parkison, C., McPhie, P., and Cheng, S. Y. (1989) Cytosolic thyroid hormone-binding protein is a monomer of pyruvate kinase. *Proc. Natl. Acad. Sci. U.S.A.* **86,** 7861–7865
105. Giallongo, A., Feo, S., Moore, R., Croce, C. M., and Showe, L. C. (1986) Molecular cloning and nucleotide sequence of a full-length cDNA for human α-enolase. *Proc. Natl. Acad. Sci. U.S.A.* **83,** 6741–6745
106. Gracy, R. W. (1975) Triose-phosphate isomerase from human erythrocytes. *Methods Enzymol.* **41,** 442–447

SUPPLEMENTAL FIGURE LEGENDS

Supplemental Figure 1: Glycolytic enzyme molecules are not externalized on autophagic or necrotic cells. HeLa cells that were induced to undergo autophagy by serum starvation with L-canavanine (1 mM) in the presence of the pan-caspase inhibitor Q-VD-OPh (10 μM), apoptotic HeLa cells (induced by serum starvation in the absence of Q-VD-OPh), and viable HeLa cells were analyzed cytofluorimetrically following staining for (**A**) α-Enolase (with polyclonal Rabbit anti- α-Enolase peptide IgG and secondary FITC-conjugated Goat ant-Rabbit IgG [Abcam]), (**B**) GAPDH (with polyclonal Rabbit anti-GAPDH IgG and secondary FITC-conjugated Goat anti-Rabbit IgG [Abcam]), and (**C**) Triosephosphate Isomerase (with polyclonal Rabbit anti-Triosephosphate Isomerase peptide IgG and secondary FITC-conjugated Goat anti-Rabbit IgG [Abcam]). Profiles shown (**A**-**C**) are for autophagic (orange, solid lines), apoptotic (solid green histograms), and viable (black, dashed lines) cells stained with the specific FITC-conjugated reagents. Cells that had lost membrane integrity (PI^+, low forward- and side-angle light scatter) were excluded from these analyses by electronic gating. Cells triggered to die necrotically also were analyzed, as in Figure 8, following staining with PE-conjugated annexin V, 7-AAD, and reagents specific (as above) for (**D**) α-Enolase, (**E**) GAPDH, and (**F**) Triosephosphate Isomerase. Cells that met the criteria of staining positively with annexin V and negatively with 7-AAD (annexin V^+ 7-AAD^-) were gated electronically, and the fluorescein signal of those cells was analyzed (shown as solid violet histograms in panels **D**-**F**). The fluorescein signal of annexin V^+ 7-AAD^- cells stained with secondary antibody alone also is presented (gray, dotted lines in panels **D**-**F**).

Supplemental Figure 2: Apoptotic externalization of glycolytic enzyme molecules is caspase-dependent. HeLa cells, subjected to irradiation with UV-C light in the presence of the pan-caspase inhibitor Q-VD-OPh (10 μM, including 90 min. pre-treatment) and in its absence, were analyzed cytofluorimetrically following staining, as in Supplementary Figure 1, for (**A**) α-Enolase, (**B**) GAPDH, and (**C**) Triosephosphate Isomerase. Profiles shown are for cells irradiated in the presence of Q-VD-OPh (blue, solid lines) and in its absence (solid green histograms). The fluorescein signal of cells stained with secondary antibody alone also is presented (gray, dotted lines). Cells that had lost membrane integrity (PI^+, low forward- and side-angle light scatter) were excluded from these analyses by electronic gating.

SUPPLEMENTAL TABLE

Supplemental Table I: Relative abundance of all apoptotic membrane-associated proteins identified by iTRAQ analysis.

	Identified Proteins	Accession ID	Ratio	T-test
1	10 kDa heat shock protein, mitochondrial	CH10_HUMAN	1.15	0.11
2	116 kDa U5 small nuclear ribonucleoprotein component	U5S1_HUMAN	1.00	1.00
3	14-3-3 protein beta/alpha	1433B_HUMAN	1.57	0.02
4	14-3-3 protein epsilon	1433E_HUMAN	1.36	0.05
5	14-3-3 protein gamma	1433G_HUMAN	0.97	0.91
6	14-3-3 protein theta	1433T_HUMAN	1.28	0.39
7	14-3-3 protein zeta/delta	1433Z_HUMAN	1.22	0.25
8	26S protease regulatory subunit 4	PRS4_HUMAN	0.84	0.04
9	26S protease regulatory subunit 6A	PRS6A_HUMAN	0.90	0.50
10	26S protease regulatory subunit 6B	PRS6B_HUMAN	0.85	0.22
11	26S protease regulatory subunit 7	PRS7_HUMAN	1.03	0.82
12	26S proteasome non-ATPase regulatory subunit 11	PSD11_HUMAN	0.96	0.79
13	26S proteasome non-ATPase regulatory subunit 13	PSD13_HUMAN	0.55	0.16
14	26S proteasome non-ATPase regulatory subunit 2	PSMD2_HUMAN	0.91	0.82
15	26S proteasome non-ATPase regulatory subunit 5	PSMD5_HUMAN	0.58	0.10
16	26S proteasome non-ATPase regulatory subunit 6	PSMD6_HUMAN	0.81	0.40
17	26S proteasome non-ATPase regulatory subunit 8	PSMD8_HUMAN	0.55	0.12
18	28S ribosomal protein S23, mitochondrial	RT23_HUMAN	0.79	0.59
19	2-oxoglutarate dehydrogenase, mitochondrial	ODO1_HUMAN	0.67	0.17
20	39S ribosomal protein L12, mitochondrial	RM12_HUMAN	0.99	0.95
21	40S ribosomal protein S10	RS10_HUMAN	0.76	0.03
22	40S ribosomal protein S11	RS11_HUMAN	0.93	0.29
23	40S ribosomal protein S12	RS12_HUMAN	0.78	0.10
24	40S ribosomal protein S13	RS13_HUMAN	0.75	0.15
25	40S ribosomal protein S14	RS14_HUMAN	0.84	0.26
26	40S ribosomal protein S15	RS15_HUMAN	0.87	0.29
27	40S ribosomal protein S15a	RS15A_HUMAN	0.68	0.01
28	40S ribosomal protein S16	RS16_HUMAN	0.68	0.05
29	40S ribosomal protein S17	RS17_HUMAN	0.52	0.00
30	40S ribosomal protein S18	RS18_HUMAN	0.66	0.04
31	40S ribosomal protein S19	RS19_HUMAN	0.78	0.02
32	40S ribosomal protein S2	RS2_HUMAN	0.57	0.03
33	40S ribosomal protein S20	RS20_HUMAN	0.88	0.47
34	40S ribosomal protein S23	RS23_HUMAN	0.57	0.01
35	40S ribosomal protein S24	RS24_HUMAN	0.81	0.11
36	40S ribosomal protein S25	RS25_HUMAN	0.84	0.17
37	40S ribosomal protein S26	RS26_HUMAN	0.94	0.61
38	40S ribosomal protein S27	RS27_HUMAN	1.07	0.29
39	40S ribosomal protein S3	RS3_HUMAN	0.87	0.20
40	40S ribosomal protein S3a	RS3A_HUMAN	0.68	0.05
41	40S ribosomal protein S4, X isoform	RS4X_HUMAN	0.81	0.05
42	40S ribosomal protein S5	RS5_HUMAN	0.67	0.11
43	40S ribosomal protein S6	RS6_HUMAN	0.78	0.10
44	40S ribosomal protein S7	RS7_HUMAN	1.07	0.55

45	40S ribosomal protein S8	RS8_HUMAN	0.84	0.03
46	40S ribosomal protein S9	RS9_HUMAN	0.68	0.01
47	40S ribosomal protein SA	RSSA_HUMAN	0.84	0.15
48	4F2 cell-surface antigen heavy chain	4F2_HUMAN	0.90	0.32
49	60 kDa heat shock protein, mitochondrial	CH60_HUMAN	1.14	0.33
50	60S acidic ribosomal protein P0	RLA0_HUMAN	0.84	0.04
51	60S acidic ribosomal protein P1	RLA1_HUMAN	0.96	0.69
52	60S acidic ribosomal protein P2	RLA2_HUMAN	0.97	0.42
53	60S ribosomal protein L10	RL10_HUMAN	0.78	0.02
54	60S ribosomal protein L10a	RL10A_HUMAN	0.73	0.14
55	60S ribosomal protein L11	RL11_HUMAN	0.94	0.61
56	60S ribosomal protein L12	RL12_HUMAN	0.81	0.08
57	60S ribosomal protein L13	RL13_HUMAN	0.71	0.02
58	60S ribosomal protein L13a	RL13A_HUMAN	0.81	0.05
59	60S ribosomal protein L14	RL14_HUMAN	0.62	0.04
60	60S ribosomal protein L15	RL15_HUMAN	0.71	0.03
61	60S ribosomal protein L17	RL17_HUMAN	0.84	0.15
62	60S ribosomal protein L18	RL18_HUMAN	0.71	0.02
63	60S ribosomal protein L18a	RL18A_HUMAN	0.81	0.05
64	60S ribosomal protein L19	RL19_HUMAN	0.45	0.03
65	60S ribosomal protein L21	RL21_HUMAN	0.78	0.02
66	60S ribosomal protein L23	RL23_HUMAN	0.71	0.05
67	60S ribosomal protein L23a	RL23A_HUMAN	0.81	0.05
68	60S ribosomal protein L24	RL24_HUMAN	0.50	0.02
69	60S ribosomal protein L26	RL26_HUMAN	0.66	0.00
70	60S ribosomal protein L27	RL27_HUMAN	0.65	0.09
71	60S ribosomal protein L27a	RL27A_HUMAN	1.03	0.71
72	60S ribosomal protein L28	RL28_HUMAN	0.87	0.11
73	60S ribosomal protein L3	RL3_HUMAN	0.73	0.05
74	60S ribosomal protein L30	RL30_HUMAN	0.93	0.29
75	60S ribosomal protein L31	RL31_HUMAN	0.87	0.29
76	60S ribosomal protein L32	RL32_HUMAN	0.58	0.01
77	60S ribosomal protein L34	RL34_HUMAN	0.56	0.04
78	60S ribosomal protein L35	RL35_HUMAN	0.73	0.01
79	60S ribosomal protein L35a	RL35A_HUMAN	0.84	0.03
80	60S ribosomal protein L36a	RL36A_HUMAN	0.59	0.00
81	60S ribosomal protein L37	RL37_HUMAN	0.81	0.11
82	60S ribosomal protein L37a	RL37A_HUMAN	0.84	0.15
83	60S ribosomal protein L4	RL4_HUMAN	0.78	0.02
84	60S ribosomal protein L5	RL5_HUMAN	0.73	0.07
85	60S ribosomal protein L6	RL6_HUMAN	0.73	0.02
86	60S ribosomal protein L7	RL7_HUMAN	0.84	0.03
87	60S ribosomal protein L7a	RL7A_HUMAN	0.78	0.02
88	60S ribosomal protein L9	RL9_HUMAN	0.60	0.02
89	6-phosphofructokinase type C	K6PP_HUMAN	0.81	0.08
90	6-phosphogluconate dehydrogenase, decarboxylating	6PGD_HUMAN	1.23	0.29
91	78 kDa glucose-regulated protein	GRP78_HUMAN	0.89	0.53
92	Acidic leucine-rich nuclear phosphoprotein 32 family member A	AN32A_HUMAN	1.19	0.03
93	Actin-related protein 2	ARP2_HUMAN	0.84	0.04
94	Actin-related protein 2/3 complex subunit 2	ARPC2_HUMAN	1.27	0.02

95	Actin-related protein 2/3 complex subunit 3	ARPC3_HUMAN	1.37	0.01
96	Actin-related protein 2/3 complex subunit 4	ARPC4_HUMAN	1.12	0.42
97	Actin-related protein 3	ARP3_HUMAN	1.19	0.31
98	Activated RNA polymerase II transcriptional coactivator p15	TCP4_HUMAN	0.87	0.20
99	Acyl-CoA-binding protein	ACBP_HUMAN	1.94	0.05
100	Adenosylhomocysteinase	SAHH_HUMAN	1.10	0.56
101	Adenylyl cyclase-associated protein 1	CAP1_HUMAN	1.23	0.18
102	ADP/ATP translocase 2	ADT2_HUMAN	0.73	0.05
103	ADP-ribosylation factor 1	ARF1_HUMAN	1.03	0.42
104	ADP-ribosylation factor 4	ARF4_HUMAN	0.87	0.29
105	ADP-ribosylation factor 6	ARF6_HUMAN	0.86	0.75
106	Alanyl-tRNA synthetase, cytoplasmic	SYAC_HUMAN	1.19	0.17
107	Aldose reductase	ALDR_HUMAN	1.68	0.02
108	Alkaline phosphatase, tissue-nonspecific isozyme	PPBT_HUMAN	0.42	0.03
109	Alpha-actinin-1	ACTN1_HUMAN	1.46	0.01
110	Alpha-actinin-4	ACTN4_HUMAN	1.18	0.22
111	Alpha-centractin	ACTZ_HUMAN	1.55	0.22
112	Alpha-enolase	ENOA_HUMAN	1.46	0.03
113	Annexin A1	ANXA1_HUMAN	0.66	0.04
114	Annexin A11	ANX11_HUMAN	1.17	0.42
115	Annexin A2	ANXA2_HUMAN	0.57	0.03
116	Annexin A3	ANXA3_HUMAN	1.16	0.51
117	Annexin A5	ANXA5_HUMAN	0.45	0.02
118	Annexin A6	ANXA6_HUMAN	0.47	0.02
119	AP-2 complex subunit beta	AP2B1_HUMAN	0.87	0.29
120	Arginyl-tRNA synthetase, cytoplasmic	SYRC_HUMAN	0.71	0.07
121	Asparagine synthetase [glutamine-hydrolyzing]	ASNS_HUMAN	0.42	0.02
122	Asparaginyl-tRNA synthetase, cytoplasmic	SYNC_HUMAN	0.90	0.32
123	Aspartate aminotransferase, mitochondrial	AATM_HUMAN	1.03	0.71
124	Aspartyl/asparaginyl beta-hydroxylase	ASPH_HUMAN	0.84	0.17
125	Aspartyl-tRNA synthetase, cytoplasmic	SYDC_HUMAN	0.68	0.01
126	ATP synthase subunit alpha, mitochondrial	ATPA_HUMAN	0.86	0.42
127	ATP synthase subunit b, mitochondrial	AT5F1_HUMAN	1.14	0.58
128	ATP synthase subunit beta, mitochondrial	ATPB_HUMAN	0.87	0.34
129	ATP synthase subunit d, mitochondrial	ATP5H_HUMAN	1.46	0.01
130	ATP synthase subunit gamma, mitochondrial	ATPG_HUMAN	0.84	0.26
131	ATPase inhibitor, mitochondrial	ATIF1_HUMAN	1.28	0.47
132	ATP-citrate synthase	ACLY_HUMAN	0.90	0.10
133	ATP-dependent DNA helicase Q1	RECQ1_HUMAN	0.57	0.14
134	ATP-dependent RNA helicase A	DHX9_HUMAN	0.84	0.04
135	ATP-dependent RNA helicase DDX39	DDX39_HUMAN	0.89	0.53
136	ATP-dependent RNA helicase DDX3X	DDX3X_HUMAN	0.93	0.29
137	Barrier-to-autointegration factor	BAF_HUMAN	0.73	0.07
138	Basic leucine zipper and W2 domain-containing protein 1	BZW1_HUMAN	0.97	0.42
139	Basigin	BASI_HUMAN	1.04	0.79
140	B-cell receptor-associated protein 31	BAP31_HUMAN	0.86	0.50
141	Bifunctional aminoacyl-tRNA synthetase	SYEP_HUMAN	0.90	0.31
142	Brain acid soluble protein 1	BASP1_HUMAN	0.87	0.34
143	BTB/POZ domain-containing protein KCTD12	KCD12_HUMAN	1.50	0.07
144	C-1-tetrahydrofolate synthase, cytoplasmic	C1TC_HUMAN	0.76	0.20

145	CAD protein	PYR1_HUMAN	0.98	0.94
146	Calmodulin	CALM_HUMAN	1.25	0.58
147	Calnexin	CALX_HUMAN	0.93	0.55
148	Calpastatin	ICAL_HUMAN	1.68	0.03
149	Calreticulin	CALR_HUMAN	0.75	0.21
150	Calumenin	CALU_HUMAN	0.73	0.01
151	Caprin-1	CAPR1_HUMAN	1.15	0.29
152	Carbamoyl-phosphate synthase [ammonia], mitochondrial	CPSM_HUMAN	0.81	0.22
153	Carbonyl reductase [NADPH] 1	CBR1_HUMAN	1.37	0.07
154	Casein kinase II subunit alpha	CSK21_HUMAN	0.90	0.09
155	Cation-dependent mannose-6-phosphate receptor	MPRD_HUMAN	0.96	0.74
156	Cation-independent mannose-6-phosphate receptor	MPRI_HUMAN	0.63	0.20
157	CD44 antigen	CD44_HUMAN	1.11	0.31
158	CD59 glycoprotein	CD59_HUMAN	0.48	0.09
159	CD9 antigen	CD9_HUMAN	0.93	0.68
160	Cell division protein kinase 1	CDK1_HUMAN	1.15	0.34
161	Cell surface glycoprotein MUC18	MUC18_HUMAN	0.81	0.32
162	Chloride intracellular channel protein 1	CLIC1_HUMAN	0.99	0.97
163	Chromobox protein homolog 3	CBX3_HUMAN	1.07	0.42
164	Citrate synthase, mitochondrial	CISY_HUMAN	0.93	0.29
165	Clathrin heavy chain 1	CLH1_HUMAN	0.75	0.15
166	Clathrin light chain A	CLCA_HUMAN	0.68	0.05
167	Clathrin light chain B	CLCB_HUMAN	0.76	0.11
168	Coatomer subunit alpha	COPA_HUMAN	1.03	0.87
169	Coatomer subunit beta	COPB_HUMAN	0.97	0.80
170	Cofilin-1	COF1_HUMAN	1.32	0.03
171	Cold shock domain-containing protein E1	CSDE1_HUMAN	1.07	0.42
172	Complement C1Q subcomponent-binding protein, mitochondrial	C1QBP_HUMAN	1.23	0.17
173	Complement decay-accelerating factor	DAF_HUMAN	0.68	0.11
174	Condensin complex subunit 1	CND1_HUMAN	0.73	0.47
175	Core histone macro-H2A.1	H2AY_HUMAN	1.00	0.42
176	Creatine kinase B-type	KCRB_HUMAN	1.37	0.37
177	Cyclin-dependent kinase inhibitor 2A, isoforms 1/2/3	CD2A1_HUMAN	1.42	0.11
178	Cystatin-B	CYTB_HUMAN	1.54	0.18
179	Cytochrome b5	CYB5_HUMAN	0.84	0.04
180	Cytochrome b-c1 complex subunit 7	QCR7_HUMAN	0.50	0.02
181	Cytochrome c	CYC_HUMAN	2.71	0.01
182	Cytoplasmic dynein 1 heavy chain 1	DYHC1_HUMAN	0.69	0.09
183	Cytosolic phospholipase A2	PA24A_HUMAN	1.46	0.01
184	D-3-phosphoglycerate dehydrogenase	SERA_HUMAN	0.97	0.71
185	D-dopachrome decarboxylase	DOPD_HUMAN	1.35	0.14
186	Delta(3,5)-Delta(2,4)-dienoyl-CoA isomerase, mitochondrial	ECH1_HUMAN	0.66	0.01
187	Deoxyuridine 5'-triphosphate nucleotidohydrolase, mitochondrial	DUT_HUMAN	1.07	0.29
188	Destrin	DEST_HUMAN	1.11	0.31
189	Dihydrolipoyl dehydrogenase, mitochondrial	DLDH_HUMAN	0.90	0.31
190	Dihydropyrimidinase-related protein 2	DPYL2_HUMAN	0.96	0.87
191	Dipeptidyl peptidase 1	CATC_HUMAN	0.31	0.02
192	DNA damage-binding protein 1	DDB1_HUMAN	0.88	0.63
193	DNA replication licensing factor MCM2	MCM2_HUMAN	1.07	0.29
194	DNA replication licensing factor MCM4	MCM4_HUMAN	0.64	0.02

195	DNA replication licensing factor MCM5	MCM5_HUMAN	0.60	0.02
196	DNA replication licensing factor MCM6	MCM6_HUMAN	1.07	0.29
197	DNA replication licensing factor MCM7	MCM7_HUMAN	0.67	0.16
198	DNA topoisomerase 1	TOP1_HUMAN	0.96	0.69
199	DNA topoisomerase 2-alpha	TOP2A_HUMAN	0.73	0.01
200	DNA-dependent protein kinase catalytic subunit	PRKDC_HUMAN	0.76	0.03
201	DnaJ homolog subfamily A member 1	DNJA1_HUMAN	1.28	0.20
202	Dolichyl-diphosphooligosac.-protein glycosyltransferase 48 kDa sub.	OST48_HUMAN	0.98	0.92
203	Dolichyl-diphosphooligosac.-protein glycosyltransferase subunit 1	RPN1_HUMAN	0.99	0.95
204	Dolichyl-diphosphooligosac.-protein glycosyltransferase subunit 2	RPN2_HUMAN	0.72	0.16
205	Dolichyl-diphosphooligosac.-protein glycosyltransferase sub. STT3B	STT3B_HUMAN	0.79	0.39
206	EGF-like repeat and discoidin I-like domain-containing protein 3	EDIL3_HUMAN	0.68	0.05
207	Elongation factor 1-alpha 1	EF1A1_HUMAN	1.00	0.42
208	Elongation factor 1-beta	EF1B_HUMAN	1.11	0.10
209	Elongation factor 1-delta	EF1D_HUMAN	1.00	1.00
210	Elongation factor 1-gamma	EF1G_HUMAN	1.19	0.04
211	Elongation factor 2	EF2_HUMAN	1.19	0.03
212	Elongation factor Tu, mitochondrial	EFTU_HUMAN	0.90	0.32
213	Emerin	EMD_HUMAN	0.88	0.53
234	Endoplasmic reticulum resident protein 29	ERP29_HUMAN	0.78	0.20
215	Endoplasmin	ENPL_HUMAN	0.84	0.17
216	Endothelin-converting enzyme 1	ECE1_HUMAN	0.62	0.04
217	Enhancer of rudimentary homolog	ERH_HUMAN	0.94	0.82
218	Equilibrative nucleoside transporter 1	S29A1_HUMAN	0.92	0.69
219	Erythrocyte band 7 integral membrane protein	STOM_HUMAN	1.07	0.55
220	Eukaryotic initiation factor 4A-I	IF4A1_HUMAN	0.97	0.42
221	Eukaryotic initiation factor 4A-III	IF4A3_HUMAN	0.97	0.71
222	Eukaryotic peptide chain release factor GTP-binding subunit ERF3A	ERF3A_HUMAN	1.27	0.02
223	Eukaryotic translation elongation factor 1 epsilon-1	MCA3_HUMAN	1.37	0.26
224	Eukaryotic translation initiation factor 1A, X-chromosomal	IF1AX_HUMAN	1.18	0.34
225	Eukaryotic translation initiation factor 2 subunit 1	IF2A_HUMAN	1.16	0.51
226	Eukaryotic translation initiation factor 2 subunit 2-like protein	IF2BL_HUMAN	0.87	0.29
227	Eukaryotic translation initiation factor 2 subunit 3	IF2G_HUMAN	0.73	0.12
228	Eukaryotic translation initiation factor 3 subunit A	EIF3A_HUMAN	1.19	0.17
229	Eukaryotic translation initiation factor 3 subunit B	EIF3B_HUMAN	0.87	0.34
230	Eukaryotic translation initiation factor 3 subunit C	EIF3C_HUMAN	0.95	0.80
231	Eukaryotic translation initiation factor 3 subunit I	EIF3I_HUMAN	0.93	0.55
232	Eukaryotic translation initiation factor 3 subunit L	EIF3L_HUMAN	1.04	0.42
233	Eukaryotic translation initiation factor 4 gamma 1	IF4G1_HUMAN	0.96	0.74
234	Eukaryotic translation initiation factor 5A-1	IF5A1_HUMAN	1.11	0.31
235	Exportin-1	XPO1_HUMAN	1.19	0.30
236	Exportin-2	XPO2_HUMAN	1.55	0.09
237	Ezrin	EZRI_HUMAN	1.32	0.03
238	FACT complex subunit SSRP1	SSRP1_HUMAN	0.57	0.13
239	F-actin-capping protein subunit beta	CAPZB_HUMAN	0.81	0.11
240	Far upstream element-binding protein 1	FUBP1_HUMAN	0.96	0.79
241	Farnesyl pyrophosphate synthase	FPPS_HUMAN	1.11	0.49
242	Fascin	FSCN1_HUMAN	1.47	0.09
243	Fatty acid synthase	FAS_HUMAN	1.23	0.00
244	Fatty aldehyde dehydrogenase	AL3A2_HUMAN	0.72	0.33

245	Filamin-A	FLNA_HUMAN	0.84	0.04
246	Filamin-B	FLNB_HUMAN	1.23	0.08
247	Flap endonuclease 1	FEN1_HUMAN	0.93	0.55
248	Fructose-bisphosphate aldolase A	ALDOA_HUMAN	1.46	0.03
249	Fumarate hydratase, mitochondrial	FUMH_HUMAN	1.37	0.07
250	Galectin-1	LEG1_HUMAN	1.17	0.42
251	Gelsolin	GELS_HUMAN	0.59	0.07
252	General transcription factor II-I	GTF2I_HUMAN	0.91	0.56
253	Glucose-6-phosphate 1-dehydrogenase	G6PD_HUMAN	0.90	0.42
254	Glucose-6-phosphate isomerase	G6PI_HUMAN	1.36	0.12
255	Glucosidase 2 subunit beta	GLU2B_HUMAN	0.76	0.07
256	Glutaminyl-tRNA synthetase	SYQ_HUMAN	1.15	0.11
257	Glutathione S-transferase Mu 3	GSTM3_HUMAN	0.81	0.32
258	Glutathione S-transferase omega-1	GSTO1_HUMAN	1.68	0.00
259	Glutathione S-transferase P	GSTP1_HUMAN	1.51	0.02
260	Glyceraldehyde-3-phosphate dehydrogenase	G3P_HUMAN	1.10	0.42
261	Glycyl-tRNA synthetase	SYG_HUMAN	0.97	0.80
262	GTP-binding nuclear protein Ran	RAN_HUMAN	1.11	0.10
263	Guanine nucleotide-binding protein G(i) subunit alpha-2	GNAI2_HUMAN	0.72	0.25
264	Guanine nucleotide-binding protein G(I)/G(S)/G(T) subunit beta-1	GBB1_HUMAN	0.68	0.05
265	Guanine nucleotide-binding protein G(s) α isoforms XLas	GNAS1_HUMAN	0.96	0.89
266	Guanine nucleotide-binding protein subunit beta-2-like 1	GBLP_HUMAN	0.73	0.07
267	Heat shock 70 kDa protein 1A/1B	HSP71_HUMAN	1.15	0.11
268	Heat shock 70 kDa protein 4	HSP74_HUMAN	1.41	0.07
269	Heat shock cognate 71 kDa protein	HSP7C_HUMAN	1.37	0.01
270	Heat shock protein 75 kDa, mitochondrial	TRAP1_HUMAN	0.96	0.69
271	Heat shock protein beta-1	HSPB1_HUMAN	0.57	0.00
272	Heat shock protein HSP 90-alpha	HS90A_HUMAN	1.68	0.05
273	Heat shock protein HSP 90-beta	HS90B_HUMAN	1.36	0.05
274	Hepatoma-derived growth factor	HDGF_HUMAN	1.32	0.20
275	Heterogeneous nuclear ribonucleoprotein A/B	ROAA_HUMAN	0.78	0.25
276	Heterogeneous nuclear ribonucleoprotein A0	ROA0_HUMAN	0.90	0.31
277	Heterogeneous nuclear ribonucleoprotein A1	ROA1_HUMAN	0.90	0.09
278	Heterogeneous nuclear ribonucleoprotein A3	ROA3_HUMAN	0.90	0.31
279	Heterogeneous nuclear ribonucleoprotein D0	HNRPD_HUMAN	0.78	0.02
280	Heterogeneous nuclear ribonucleoprotein D-like	HNRDL_HUMAN	0.97	0.42
281	Heterogeneous nuclear ribonucleoprotein F	HNRPF_HUMAN	0.87	0.33
282	Heterogeneous nuclear ribonucleoprotein G	HNRPG_HUMAN	0.73	0.01
283	Heterogeneous nuclear ribonucleoprotein H	HNRH1_HUMAN	1.00	0.98
284	Heterogeneous nuclear ribonucleoprotein H3	HNRH3_HUMAN	0.78	0.10
285	Heterogeneous nuclear ribonucleoprotein K	HNRPK_HUMAN	0.79	0.12
286	Heterogeneous nuclear ribonucleoprotein L	HNRPL_HUMAN	0.81	0.05
287	Heterogeneous nuclear ribonucleoprotein M	HNRPM_HUMAN	0.87	0.20
288	Heterogeneous nuclear ribonucleoprotein Q	HNRPQ_HUMAN	1.03	0.42
289	Heterogeneous nuclear ribonucleoprotein R	HNRPR_HUMAN	0.78	0.02
290	Heterogeneous nuclear ribonucleoprotein U	HNRPU_HUMAN	0.93	0.29
291	Heterogeneous nuclear ribonucleoproteins A2/B1	ROA2_HUMAN	0.71	0.00
292	Heterogeneous nuclear ribonucleoproteins C1/C2	HNRPC_HUMAN	0.73	0.02
293	High mobility group protein B1	HMGB1_HUMAN	1.37	0.07
294	High mobility group protein B2	HMGB2_HUMAN	1.11	0.31

295	High mobility group protein HMG-I/HMG-Y	HMGA1_HUMAN	0.84	0.17
296	Histone H1.4	H14_HUMAN	0.69	0.09
297	Histone H1.5	H15_HUMAN	0.64	0.02
298	Histone H2A type 2-B	H2A2B_HUMAN	0.28	0.01
299	Histone H2A.V	H2AV_HUMAN	0.84	0.03
300	Histone H2B type 1-J	H2B1J_HUMAN	0.64	0.01
301	Histone H3.1t	H31T_HUMAN	0.87	0.00
302	Histone H4	H4_HUMAN	0.76	0.07
303	HLA class I histocompatibility antigen, A-68 alpha chain	1A68_HUMAN	0.84	0.17
304	HLA class I histocompatibility antigen, B-15 alpha chain	1B15_HUMAN	1.35	0.22
305	Hsc70-interacting protein	F10A1_HUMAN	1.15	0.11
306	Hypoxia up-regulated protein 1	HYOU1_HUMAN	0.90	0.09
307	Importin subunit alpha-1	IMA1_HUMAN	1.14	0.65
308	Importin subunit beta-1	IMB1_HUMAN	1.19	0.03
309	Importin-5	IPO5_HUMAN	1.41	0.07
310	Importin-7	IPO7_HUMAN	1.52	0.01
311	Inorganic pyrophosphatase	IPYR_HUMAN	1.12	0.61
312	Inosine-5'-monophosphate dehydrogenase 2	IMDH2_HUMAN	1.03	0.80
313	Integrin alpha-11	ITA11_HUMAN	1.03	0.82
314	Integrin alpha-3	ITA3_HUMAN	1.43	0.24
315	Integrin beta-1	ITB1_HUMAN	1.07	0.29
316	Interleukin enhancer-binding factor 2	ILF2_HUMAN	0.68	0.03
317	Interleukin enhancer-binding factor 3	ILF3_HUMAN	0.64	0.04
318	Isocitrate dehydrogenase [NADP] cytoplasmic	IDHC_HUMAN	1.21	0.45
319	Isoleucyl-tRNA synthetase, cytoplasmic	SYIC_HUMAN	1.03	0.88
320	Keratin, type I cytoskeletal 10	K1C10_HUMAN	0.54	0.04
321	Keratin, type I cytoskeletal 17	K1C17_HUMAN	0.51	0.14
322	Keratin, type I cytoskeletal 18	K1C18_HUMAN	0.93	0.55
323	Keratin, type I cytoskeletal 9	K1C9_HUMAN	0.98	0.94
324	Keratin, type II cytoskeletal 1	K2C1_HUMAN	0.84	0.42
325	Keratin, type II cytoskeletal 2 epidermal	K22E_HUMAN	0.74	0.14
326	Keratin, type II cytoskeletal 7	K2C7_HUMAN	0.68	0.09
327	Keratin, type II cytoskeletal 8	K2C8_HUMAN	0.64	0.04
328	KH domain-containing RNA-binding signal trans.-assoc. protein 1	KHDR1_HUMAN	0.86	0.46
329	Kynureninase	KYNU_HUMAN	1.40	0.29
330	Lamin-A/C	LMNA_HUMAN	0.73	0.07
331	Lamin-B1	LMNB1_HUMAN	0.90	0.32
332	LanC-like protein 1	LANC1_HUMAN	0.72	0.30
333	Large neutral amino acids transporter small subunit 1	LAT1_HUMAN	0.29	0.03
334	Leucine-rich PPR motif-containing protein, mitochondrial	LPPRC_HUMAN	1.22	0.56
335	Leucine-rich repeat-containing protein 59	LRC59_HUMAN	0.93	0.68
336	Leucyl-tRNA synthetase, cytoplasmic	SYLC_HUMAN	0.90	0.31
337	LIM domain and actin-binding protein 1	LIMA1_HUMAN	0.90	0.31
338	L-lactate dehydrogenase A chain	LDHA_HUMAN	1.32	0.04
339	L-lactate dehydrogenase B chain	LDHB_HUMAN	1.23	0.17
340	Lupus La protein	LA_HUMAN	1.04	0.42
341	Lysosome-associated membrane glycoprotein 1	LAMP1_HUMAN	0.66	0.01
342	Lysyl-tRNA synthetase	SYK_HUMAN	1.07	0.29
343	Macrophage migration inhibitory factor	MIF_HUMAN	2.00	0.01
344	Malate dehydrogenase, mitochondrial	MDHM_HUMAN	1.19	0.15

345	Matrin-3	MATR3_HUMAN	0.73	0.49
346	Membrane-associated progesterone receptor component 2	PGRC2_HUMAN	0.90	0.50
347	Methionyl-tRNA synthetase, cytoplasmic	SYMC_HUMAN	0.90	0.32
348	Microsomal glutathione S-transferase 1	MGST1_HUMAN	0.81	0.08
349	Microtubule-associated protein RP/EB family member 1	MARE1_HUMAN	1.02	0.92
350	Mitochondrial carrier homolog 2	MTCH2_HUMAN	0.66	0.01
351	Mitochondrial inner membrane protein	IMMT_HUMAN	1.24	0.22
352	Moesin	MOES_HUMAN	1.03	0.87
353	Monocarboxylate transporter 1	MOT1_HUMAN	1.03	0.71
354	Monocarboxylate transporter 4	MOT4_HUMAN	0.92	0.64
355	mRNA turnover protein 4 homolog	MRT4_HUMAN	0.99	0.95
356	Multidrug resistance-associated protein 1	MRP1_HUMAN	0.74	0.41
357	Multifunctional protein ADE2	PUR6_HUMAN	0.91	0.56
358	Myb-binding protein 1A	MBB1A_HUMAN	0.84	0.62
359	Myoferlin	MYOF_HUMAN	0.69	0.15
360	Myosin light polypeptide 6	MYL6_HUMAN	0.73	0.02
361	Myosin regulatory light chain 12A	ML12A_HUMAN	0.74	0.35
362	Myosin-10	MYH10_HUMAN	1.03	0.71
363	Myosin-9	MYH9_HUMAN	0.90	0.42
364	Myristoylated alanine-rich C-kinase substrate	MARCS_HUMAN	1.52	0.05
365	N-acetylgalactosaminyltransferase 7	GALT7_HUMAN	0.68	0.01
366	NAD(P) transhydrogenase, mitochondrial	NNTM_HUMAN	0.94	0.42
367	NAD(P)H dehydrogenase [quinone] 1	NQO1_HUMAN	0.81	0.22
368	NADH dehydrogenase [ubiquinone] 1 alpha subcomplex subunit 4	NDUA4_HUMAN	0.83	0.42
369	NADH-cytochrome b5 reductase 3	NB5R3_HUMAN	1.15	0.17
370	Nascent polypeptide-associated complex subunit alpha	NACA_HUMAN	1.37	0.01
371	Neuroblast differentiation-associated protein AHNAK	AHNK_HUMAN	1.00	0.98
372	Neuroplastin	NPTN_HUMAN	0.76	0.11
373	Neutral alpha-glucosidase AB	GANAB_HUMAN	0.96	0.74
374	Neutral amino acid transporter B(0)	AAAT_HUMAN	1.10	0.75
375	Niban-like protein 1	NIBL1_HUMAN	1.34	0.30
376	Non-POU domain-containing octamer-binding protein	NONO_HUMAN	0.62	0.01
377	Non-specific lipid-transfer protein	NLTP_HUMAN	0.66	0.14
378	Nuclear migration protein nudC	NUDC_HUMAN	1.46	0.01
379	Nuclear pore complex protein Nup155	NU155_HUMAN	0.75	0.32
380	Nuclear pore complex protein Nup205	NU205_HUMAN	0.79	0.21
381	Nuclear ubiquitous casein and cyclin-dependent kinases substrate	NUCKS_HUMAN	0.80	0.37
382	Nuclease-sensitive element-binding protein 1	YBOX1_HUMAN	0.82	0.48
383	Nucleolar RNA helicase 2	DDX21_HUMAN	1.27	0.18
384	Nucleolin	NUCL_HUMAN	0.84	0.04
385	Nucleophosmin	NPM_HUMAN	1.11	0.10
386	Nucleoside diphosphate kinase A	NDKA_HUMAN	1.23	0.08
387	Nucleoside diphosphate kinase B	NDKB_HUMAN	1.62	0.03
388	Nucleosome assembly protein 1-like 1	NP1L1_HUMAN	1.28	0.10
389	PC4 and SFRS1-interacting protein	PSIP1_HUMAN	0.78	0.10
390	Peptidyl-prolyl cis-trans isomerase A	PPIA_HUMAN	1.74	0.00
391	Peptidyl-prolyl cis-trans isomerase B	PPIB_HUMAN	0.75	0.15
392	Peptidyl-prolyl cis-trans isomerase FKBP10	FKB10_HUMAN	0.96	0.69
393	Peptidyl-prolyl cis-trans isomerase FKBP4	FKBP4_HUMAN	1.37	0.14
394	Peroxiredoxin-1	PRDX1_HUMAN	0.87	0.33

395	Peroxiredoxin-2	PRDX2_HUMAN	0.71	0.00
396	Peroxiredoxin-4	PRDX4_HUMAN	1.15	0.29
397	Peroxiredoxin-5, mitochondrial	PRDX5_HUMAN	1.08	0.58
398	Peroxiredoxin-6	PRDX6_HUMAN	1.41	0.07
399	Phosphoglycerate kinase 1	PGK1_HUMAN	1.46	0.03
400	Phosphoglycerate mutase 1	PGAM1_HUMAN	1.19	0.04
401	Plasminogen activator inhibitor 1 RNA-binding protein	PAIRB_HUMAN	0.92	0.64
402	Plastin-3	PLST_HUMAN	1.62	0.01
403	Platelet-activating factor acetylhydrolase IB subunit beta	PA1B2_HUMAN	0.92	0.78
404	Plectin	PLEC_HUMAN	1.11	0.32
405	Podocalyxin	PODXL_HUMAN	0.79	0.12
406	Poly [ADP-ribose] polymerase 1	PARP1_HUMAN	0.75	0.15
407	Poly(rC)-binding protein 2	PCBP2_HUMAN	0.97	0.80
408	Polyadenylate-binding protein 1	PABP1_HUMAN	1.00	1.00
409	Polypeptide N-acetylgalactosaminyltransferase 2	GALT2_HUMAN	0.62	0.00
410	Polypyrimidine tract-binding protein 1	PTBP1_HUMAN	1.03	0.87
411	Pre-mRNA-processing factor 19	PRP19_HUMAN	0.93	0.29
412	Pre-mRNA-processing-splicing factor 8	PRP8_HUMAN	0.66	0.08
413	Probable ATP-dependent RNA helicase DDX17	DDX17_HUMAN	0.66	0.01
434	Probable ATP-dependent RNA helicase DDX5	DDX5_HUMAN	0.86	0.51
415	Procollagen galactosyltransferase 1	GT251_HUMAN	0.54	0.10
416	Profilin-1	PROF1_HUMAN	1.80	0.01
417	Programmed cell death 6-interacting protein	PDC6I_HUMAN	1.47	0.17
418	Programmed cell death protein 6	PDCD6_HUMAN	0.59	0.03
419	Prohibitin-2	PHB2_HUMAN	1.23	0.08
420	Proliferating cell nuclear antigen	PCNA_HUMAN	1.01	0.97
421	Proliferation-associated protein 2G4	PA2G4_HUMAN	1.19	0.03
422	Prostaglandin E synthase 3	TEBP_HUMAN	0.93	0.00
423	Prostaglandin F2 receptor negative regulator	FPRP_HUMAN	0.93	0.00
424	Proteasome activator complex subunit 2	PSME2_HUMAN	1.04	0.69
425	Proteasome activator complex subunit 3	PSME3_HUMAN	0.67	0.14
426	Proteasome subunit alpha type-3	PSA3_HUMAN	1.08	0.58
427	Proteasome subunit alpha type-4	PSA4_HUMAN	0.81	0.32
428	Proteasome subunit alpha type-5	PSA5_HUMAN	1.32	0.00
429	Proteasome subunit alpha type-6	PSA6_HUMAN	0.86	0.46
430	Proteasome subunit beta type-3	PSB3_HUMAN	1.36	0.05
431	Protein disulfide-isomerase	PDIA1_HUMAN	0.78	0.20
432	Protein disulfide-isomerase A3	PDIA3_HUMAN	0.90	0.32
433	Protein disulfide-isomerase A4	PDIA4_HUMAN	0.87	0.11
434	Protein disulfide-isomerase A6	PDIA6_HUMAN	0.90	0.32
435	Protein ERGIC-53	LMAN1_HUMAN	0.69	0.05
436	Protein S100-A10	S10AA_HUMAN	0.61	0.03
437	Protein S100-A11	S10AB_HUMAN	0.87	0.34
438	Protein S100-A4	S10A4_HUMAN	0.57	0.03
439	Protein S100-A6	S10A6_HUMAN	1.07	0.29
440	Protein SET	SET_HUMAN	1.19	0.04
441	Protein transport protein Sec31A	SC31A_HUMAN	0.60	0.02
442	Puromycin-sensitive aminopeptidase	PSA_HUMAN	1.10	0.56
443	Put. pre-mRNA-splicing factor ATP-dependent RNA helicase DHX15	DHX15_HUMAN	0.87	0.00
444	Putative RNA-binding protein Luc7-like 2	LC7L2_HUMAN	0.71	0.07

445	Pyruvate carboxylase, mitochondrial	PYC_HUMAN	0.85	0.71
446	Pyruvate dehydrogenase E1 component subunit beta, mitochondrial	ODPB_HUMAN	0.87	0.00
447	Pyruvate kinase isozymes M1/M2	KPYM_HUMAN	1.11	0.09
448	Radixin	RADI_HUMAN	0.81	0.32
449	Ran-specific GTPase-activating protein	RANG_HUMAN	1.52	0.08
450	Ras GTPase-activating protein-binding protein 1	G3BP1_HUMAN	0.97	0.82
451	Ras GTPase-activating-like protein IQGAP1	IQGA1_HUMAN	1.06	0.70
452	Ras-related protein Rab-1B	RAB1B_HUMAN	1.28	0.02
453	Ras-related protein Rab-2A	RAB2A_HUMAN	1.23	0.18
454	Ras-related protein Rab-7a	RAB7A_HUMAN	0.87	0.29
455	Ras-related protein Ral-A	RALA_HUMAN	1.07	0.68
456	Ras-related protein Rap-1b	RAP1B_HUMAN	0.79	0.39
457	Replication protein A 70 kDa DNA-binding subunit	RFA1_HUMAN	1.23	0.11
458	Reticulocalbin-1	RCN1_HUMAN	0.75	0.15
459	Reticulon-3	RTN3_HUMAN	0.90	0.32
460	Reticulon-4	RTN4_HUMAN	0.71	0.02
461	Rho GDP-dissociation inhibitor 1	GDIR1_HUMAN	1.42	0.11
462	Ribonucleoside-diphosphate reductase large subunit	RIR1_HUMAN	1.11	0.32
463	Ribose-phosphate pyrophosphokinase 1	PRPS1_HUMAN	0.82	0.18
464	Ribosomal protein S6 kinase alpha-1	KS6A1_HUMAN	0.71	0.07
465	Ribosome-binding protein 1	RRBP1_HUMAN	1.27	0.18
466	RNA-binding protein 8A	RBM8A_HUMAN	1.07	0.29
467	RNA-binding protein FUS	FUS_HUMAN	0.87	0.33
468	RNA-binding protein Musashi homolog 2	MSI2H_HUMAN	0.71	0.36
469	rRNA 2'-O-methyltransferase fibrillarin	FBRL_HUMAN	0.75	0.30
470	RuvB-like 1	RUVB1_HUMAN	0.97	0.71
471	RuvB-like 2	RUVB2_HUMAN	1.03	0.42
472	Sarcoplasmic/endoplasmic reticulum calcium ATPase 2	AT2A2_HUMAN	1.11	0.32
473	Septin-7	SEPT7_HUMAN	1.12	0.75
474	Serine hydroxymethyltransferase, mitochondrial	GLYM_HUMAN	0.92	0.64
475	Serine/threonine-protein phosphatase PP1-beta catalytic subunit	PP1B_HUMAN	0.72	0.23
476	Serine-threonine kinase receptor-associated protein	STRAP_HUMAN	1.11	0.32
477	Serpin H1	SERPH_HUMAN	0.81	0.05
478	Signal recognition particle 14 kDa protein	SRP14_HUMAN	0.92	0.69
479	Signal recognition particle 9 kDa protein	SRP09_HUMAN	0.84	0.04
480	Single-stranded DNA-binding protein, mitochondrial	SSBP_HUMAN	0.90	0.32
481	Small nuclear ribonucleoprotein G-like protein	RUXGL_HUMAN	0.79	0.44
482	Small nuclear ribonucleoprotein Sm D3	SMD3_HUMAN	0.61	0.03
483	Small nuclear ribonucleoprotein-associated proteins B and B'	RSMB_HUMAN	0.32	0.03
484	Sodium- and chloride-dependent taurine transporter	SC6A6_HUMAN	1.46	0.09
485	Sodium/potassium-transporting ATPase subunit alpha-1	AT1A1_HUMAN	1.00	0.97
486	Sodium/potassium-transporting ATPase subunit beta-1	AT1B1_HUMAN	1.18	0.22
487	Sodium/potassium-transporting ATPase subunit beta-3	AT1B3_HUMAN	0.84	0.17
488	Solute carrier family 2, facilitated glucose transporter member 1	GTR1_HUMAN	0.74	0.33
489	Sorcin	SORCN_HUMAN	0.92	0.69
490	Spectrin alpha chain, brain	SPTA2_HUMAN	0.97	0.42
491	Spectrin beta chain, brain 1	SPTB2_HUMAN	1.46	0.01
492	S-phase kinase-associated protein 1	SKP1_HUMAN	0.97	0.42
493	Splicing factor 3B subunit 2	SF3B2_HUMAN	0.97	0.71
494	Splicing factor 3B subunit 3	SF3B3_HUMAN	0.91	0.56

495	Splicing factor U2AF 65 kDa subunit	U2AF2_HUMAN	0.50	0.18
496	Splicing factor, arginine/serine-rich 1	SFRS1_HUMAN	0.81	0.11
497	Splicing factor, arginine/serine-rich 6	SFRS6_HUMAN	0.66	0.01
498	Splicing factor, proline- and glutamine-rich	SFPQ_HUMAN	0.84	0.03
499	Staphylococcal nuclease domain-containing protein 1	SND1_HUMAN	0.91	0.64
500	Stathmin	STMN1_HUMAN	2.07	0.00
501	Stress-70 protein, mitochondrial	GRP75_HUMAN	0.90	0.42
502	Stress-induced-phosphoprotein 1	STIP1_HUMAN	1.23	0.08
503	Succinate dehydrogenase [ubiquinone] flavoprotein subunit, mito	DHSA_HUMAN	0.93	0.00
504	Succinyl-CoA:3-ketoacid-coenzyme A transferase 1, mitochondrial	SCOT1_HUMAN	0.78	0.20
505	SUMO-conjugating enzyme UBC9	UBC9_HUMAN	1.81	0.02
506	Superoxide dismutase [Cu-Zn]	SODC_HUMAN	1.36	0.05
507	Syndecan-2	SDC2_HUMAN	1.36	0.12
508	Talin-1	TLN1_HUMAN	1.07	0.42
509	T-complex protein 1 subunit alpha	TCPA_HUMAN	0.84	0.15
510	T-complex protein 1 subunit delta	TCPD_HUMAN	1.19	0.30
511	T-complex protein 1 subunit epsilon	TCPE_HUMAN	1.74	0.01
512	T-complex protein 1 subunit eta	TCPH_HUMAN	1.43	0.18
513	T-complex protein 1 subunit gamma	TCPG_HUMAN	1.32	0.04
534	T-complex protein 1 subunit theta	TCPQ_HUMAN	1.46	0.03
515	T-complex protein 1 subunit zeta	TCPZ_HUMAN	1.00	0.98
516	Thioredoxin	THIO_HUMAN	1.56	0.03
517	Thioredoxin domain-containing protein 17	TXD17_HUMAN	1.47	0.17
518	Thioredoxin domain-containing protein 5	TXND5_HUMAN	0.97	0.80
519	Threonyl-tRNA synthetase, cytoplasmic	SYTC_HUMAN	1.07	0.42
520	Thymidylate kinase	KTHY_HUMAN	0.81	0.05
521	Trans-2,3-enoyl-CoA reductase	TECR_HUMAN	0.64	0.08
522	Transcription factor BTF3	BTF3_HUMAN	0.91	0.64
523	Transferrin receptor protein 1	TFR1_HUMAN	0.93	0.29
524	Transformer-2 protein homolog beta	TRA2B_HUMAN	0.79	0.18
525	Transforming protein RhoA	RHOA_HUMAN	1.19	0.42
526	Transgelin	TAGL_HUMAN	1.32	0.03
527	Transgelin-2	TAGL2_HUMAN	1.68	0.05
528	Transitional endoplasmic reticulum ATPase	TERA_HUMAN	0.94	0.70
529	Transketolase	TKT_HUMAN	0.96	0.69
530	Translationally-controlled tumor protein	TCTP_HUMAN	1.64	0.11
531	Translocon-associated protein subunit alpha	SSRA_HUMAN	0.73	0.12
532	Transmembrane protein 97	TMM97_HUMAN	1.27	0.08
533	Transportin-1	TNPO1_HUMAN	1.34	0.28
534	Trifunctional enzyme subunit alpha, mitochondrial	ECHA_HUMAN	0.81	0.05
535	Trifunctional purine biosynthetic protein adenosine-3	PUR2_HUMAN	0.86	0.42
536	Triosephosphate isomerase	TPIS_HUMAN	1.36	0.05
537	Tripeptidyl-peptidase 2	TPP2_HUMAN	0.92	0.78
538	tRNA (cytosine-5-)-methyltransferase NSUN2	NSUN2_HUMAN	1.28	0.52
539	Tropomyosin alpha-3 chain	TPM3_HUMAN	1.19	0.15
540	Tropomyosin alpha-4 chain	TPM4_HUMAN	1.11	0.10
541	Trypsin-2	TRY2_HUMAN	0.70	0.11
542	Tryptophanyl-tRNA synthetase, cytoplasmic	SYWC_HUMAN	1.04	0.79
543	Tubulin alpha-4A chain	TBA4A_HUMAN	0.71	0.22
544	Tubulin beta chain	TBB5_HUMAN	0.76	0.00

545	Tubulin beta-2C chain	TBB2C_HUMAN	0.76	0.11
546	Tubulin beta-4 chain	TBB4_HUMAN	0.60	0.05
547	Tubulin--tyrosine ligase-like protein 12	TTL12_HUMAN	1.18	0.52
548	Tyrosine-protein kinase BAZ1B	BAZ1B_HUMAN	0.78	0.46
549	Tyrosyl-tRNA synthetase, cytoplasmic	SYYC_HUMAN	1.36	0.05
550	U1 small nuclear ribonucleoprotein 70 kDa	RU17_HUMAN	0.93	0.55
551	U2 small nuclear ribonucleoprotein A'	RU2A_HUMAN	1.00	1.00
552	U5 small nuclear ribonucleoprotein 200 kDa helicase	U520_HUMAN	1.00	1.00
553	Ubiquitin-40S ribosomal protein S27a	RS27A_HUMAN	1.82	0.08
554	Ubiquitin-like modifier-activating enzyme 1	UBA1_HUMAN	1.36	0.05
555	UPF0556 protein C19orf10	CS010_HUMAN	0.40	0.07
556	Vesicle-trafficking protein SEC22b	SC22B_HUMAN	1.03	0.71
557	Vesicular integral-membrane protein VIP36	LMAN2_HUMAN	0.82	0.25
558	Vigilin	VIGLN_HUMAN	0.76	0.03
559	Vimentin	VIME_HUMAN	1.03	0.71
560	Voltage-dependent anion-selective channel protein 1	VDAC1_HUMAN	0.93	0.58
561	Voltage-dependent anion-selective channel protein 2	VDAC2_HUMAN	0.84	0.17
562	WD repeat-containing protein 1	WDR1_HUMAN	1.37	0.23
563	X-ray repair cross-complementing protein 5	XRCC5_HUMAN	0.68	0.03
564	X-ray repair cross-complementing protein 6	XRCC6_HUMAN	0.87	0.11

The relative abundance of all 564 proteins identified in the comparative iTRAQ analysis of apoptotic and viable membrane vesicles are listed.

Supplemental Figure 1: Glycolytic enzyme molecules are not externalized on autophagic or necrotic cells.

α-Enolase | Glyceraldehyde 3-Phosphate Dehydrogenase (GAPDH) | Triosephophate Isomerase (TPI)

A. **B.** **C.**

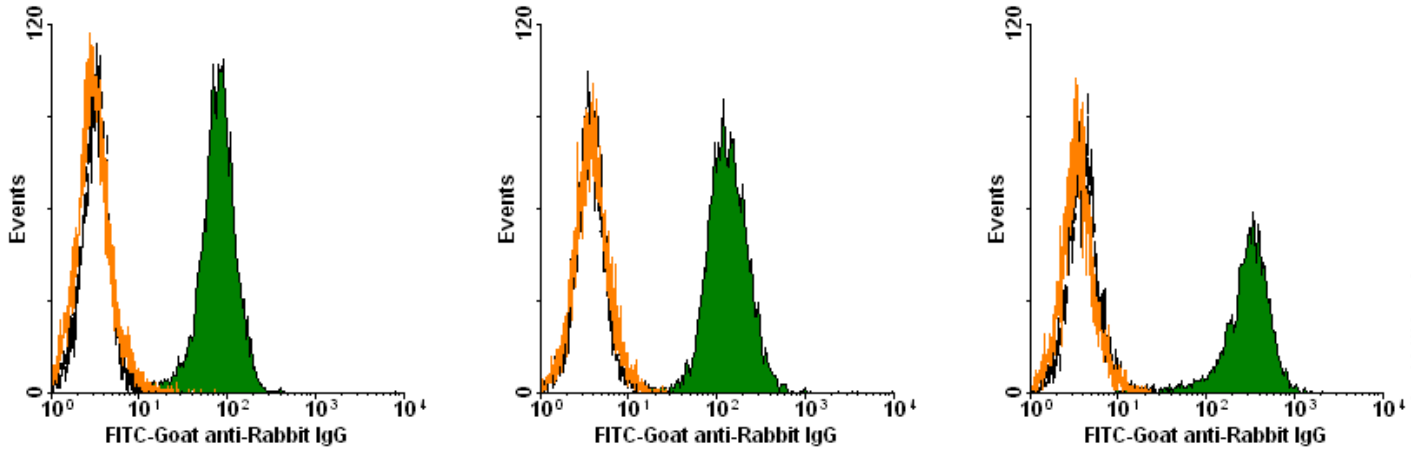

D. **E.** **F.**

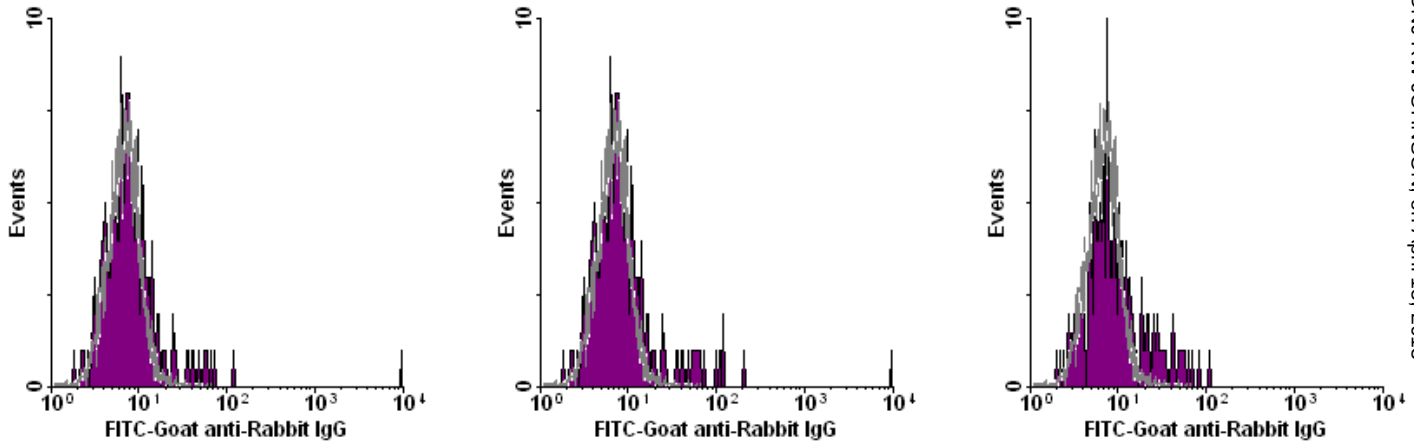

Supplemental Figure 2: Apoptotic externalization of glycolytic enzyme molecules is caspase-dependent.

A. α-Enolase

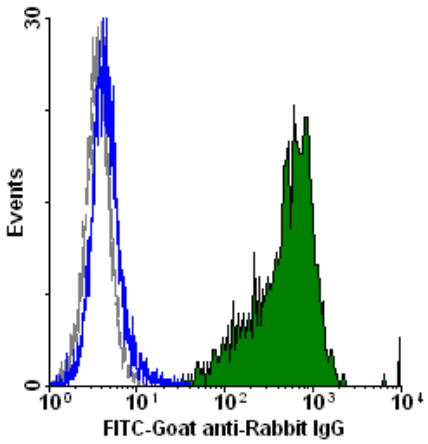

B. Glyceraldehyde 3-Phosphate Dehydrogenase (GAPDH)

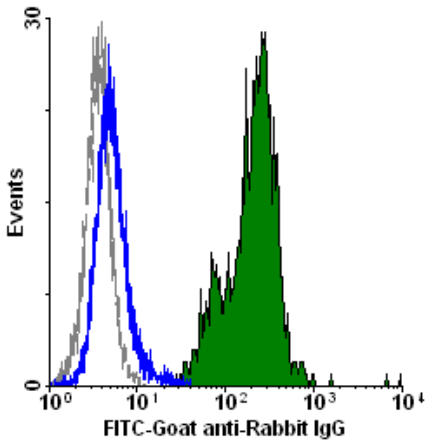

C. Triosephophate Isomerase (TPI)